MDPI

Article

Mathematical analysis of MHD non-Newtonian flow of fluid through a vertical cylinder in a drainage system by using the LNN-GNDO-SQP algorithm

Naveed Ahmad Khan [1], M Sulaiman *[1], Seyedali Mirjalili [2], Abdulah Jeza Aljohani[3,4]

[1]Department of Mathematics, Abdul Wali Khan University, Mardan 23200, KP, Pakistan (e-mail: msulaiman@awkum.edu.pk, naveedahmed146@yahoo.com)
[2]Centre for Artificial Intelligence Research and Optimisation, Torrens University Australia, Fortitude Valley, Brisbane, 4006 QLD, Australia (e-mail: ali.mirjalili@gmail.com)
[3]Department of Electrical and Computer Engineering, King Abdulaziz University, Jeddah 21589, Saudi Arabia (e-mail: ajaljohani@kau.edu.sa)
[4]Center of Excellence in Intelligent Engineering Systems, King Abdulaziz University, Jeddah 21589, Saudi Arabia

* Correspondence:sulaiman513@yahoo.co.uk

Version December 31, 2020 submitted to Journal Not Specified

Abstract: In this paper, the steady thin film flow of Johnson Segalman fluid on the surface of an infinitely long vertical cylinder used in the drainage system has been studied. Non-Newtonian Johnson Segalman fluid is mathematically modeled using the law of conservation of mass, momentum and sufficient boundary conditions that result in partial differential equations. The drainage problem is further reduced to a nonlinear ordinary differential equation by using similarity transformation. Furthermore, a new soft computing paradigm is designed. An approximate series solution is constructed using Legendre polynomials and a Legendre polynomial-based artificial neural networks architecture (LNN) to approximate the solutions for drainage problems. Training of designed neurons in LNN is carried out by hybridizing generalized normal distribution optimization (GNDO) algorithm and sequential quadratic programming (SQP). To investigate the capabilities of the proposed LNN-GNDO-SQP, we have studied the effect of variations in various non-Newtonian parameters like Stokes number (S_t), Weissenberg number (W_e), slip parameters (a), and the ratio of viscosities (ϕ). To validate our proposed technique's efficiency, solutions and absolute errors are compared with reference solutions calculated by RK-4 (ode45) and Genetic algorithm-Active set algorithm (GA-ASA). Graphical and statistical analysis of performance indicators in term of absolute errors, mean, median, standard deviation, mean absolute deviation, Theil's inequality coefficient (TIC), and error in Nash Sutcliffe efficiency (ENSE) are investigated along with global variations that further establishes the worth of LNN-GNDO-SQP algorithm in solving drainage problem.

Keywords: Lifting and drainage problems, MHD fluid, Johnson–Segalman model, Computational fluid dynamics, Weighted Legendre neural networks, Hybrid Soft Computing, Generalized normal distribution optimization, Sequential quadratic programming

1. Introduction

In recent times, steady thin film flow of magnetohydrodynamic (MHD) non-Newtonian fluids has attained researchers' interest due to their extensive use in engineering, industries, science, and technologies. Thin-film flow of Newtonian fluid was studied by Young and Munson in 1994 [1]. Landau and Lifshitz [2] in 1989 for the first time discuss thin-film flow for the drainage problem.

Siddiquie [3] found analytical results for drainage problem of fourth graded fluid over a vertical cylinder and also calculated exact solutions for Phan Thein Tanner (PTT) fluid for lifting and drainage problems [4]. Alam [5] studied thin-film flow of magnetohydrodynamic (MHD) Johnson–Segalman fluid on vertical surfaces.

Various models of fluids explain the non-Newtonian behavior of fluids. However, Johnson–Segalman fluid has gained many researchers' interest because it includes exceptional cases of classical Newtonian fluid like Oldroyd B fluid and Maxwell fluid [6]. The Johnson–Segalman fluid model is considered a viscoelastic model developed to allow non-affine deformations [7]. Many researchers discuss spurt phenomena of this non Newtonian fluid model [8–10]. Rao [11] investigated the flow of Johnson–Segalman fluid model with and without suction on rotating coaxial cylinders. Rajagopal [12] studied three different cylindrical Poiseuille flows of Johnson–Segalman fluid. Unlike most other fluid models, Johnson–Segalman fluid allows a nonmonotonic relationship between the rate of share and shear stress in a simple shear flow for different material parameters. T. Hayat [13] used the concept of this model for peristaltic flow.

Nonlinear differential equations are used in diverse areas of physics, science, and technology to model different physical problems. Generally, finding a solution to such a real-world problem is always a challenging task. Theoretical researchers in mathematics have developed various methods to find analytical expressions and approximate solutions with proven convergence for nonlinear differential equations. Adomian decomposition methods (ADM) [14,15], Variational iteration method (VIM) [16] , Finite difference method (FDM) [17,18] and Optimal homotopy perturbation method (OHAM) [19,20] are used to solve variety of ordinary and partial differential equation models. GM Sobamowo [21] used Galerkin's weighted residuals method to present an approximate solution for heat transfer in a pipe with Johnson-Segalman fluid. The motion of Johnson–Segalman fluid in an inclined channel subject to radiative flux was studied by Hayat [22] using the perturbation method. In terms of consistency, convergence, robustness, and applicability, all of these implemented techniques have their advantages and limitations. These methods are based on well established deterministic procedures. On the other hand, soft computing techniques based on neural networks are relatively less exploited and rapidly convergent in obtaining a solution to non-linear differential equations.

Stochastic intelligent computational techniques or learning algorithms based on artificial neural networks (ANN's) are optimized with novel metaheuristic and heuristic techniques that are used to solve various real-world problem, including nonlinear dusty plasma system [23], temperature profiles in longitudinal fin [24], Secondary oil recovery process [25], diabetic retinopathy classification using Fundus Images [26] and corneal model for eye surgery [27]. Recent developments in stochastic algorithms for such problems motivated authors to explore and exploit machine learning algorithms' ability to solve non-linear drainage problems.

Salient features of the presented study are summarized as follows

• The Mathematical formulation for non Newtonian Johnson-Segalman fluid is presented using the law of conservation of mass and momentum under sufficient boundary conditions that result in partial differential equations. The drainage problem is further reduced to non-linear ordinary differential equation employing similarity transformation.

• This study aims to introduce a novel solution computing that involves Legendre artificial neural networks and two algorithms: generalized normal distribution optimization (GNDO) and sequential quadratic programming (SQP). GNDO is used as a global search technique while SQP is utilized as a local search algorithm.

• Effect of variations in different parameters like Weissenberg number (W_e), Stokes number (S_t), slip parameter (a) and the ratio of viscosities (ϕ) on velocity profile of steady thin film flow of non-Newtonian Johnson-Segalman fluid is investigated.

• Performance indicators are used for different cases of drainage problem studied in this paper to validate the efficiency and correctness of the LNN-GNDO-SQP algorithm.

• Extensive statistical and graphical analysis in terms of absolute errors, fitness evaluation, MAD,

RMSE, TIC, and ENSE are provided, that demonstrated the ability of our proposed algorithm in solving real-world problems.

Nomenclature

Abbreviation	Description	Abbreviation	Description
LNN	Legendre Neural Networks	S_t	Stokes Number
GNDO	Generalized Normal Distribution Optimization	a	Slip Parameter
SQP	Sequential Quadratic Programming	ϕ	Ratio of Viscosities
ANN	Artificial Neural Networks	$\underline{V}$	Velocity Vector
MAD	Mean Absolute Deviation	ρ	Density
TIC	Theil's inequality coefficient	σ	Cauchy Stress Tensor
NSE	Nash Sutcliffe Efficiency	μ, η	Viscosities
ENSE	Error In Nash Sutcliffe Efficiency	u^t	Trial vector
RMSE	Root Mean Square Error	δ	Thinkness of Thin Film
MHD	Magnetohydrodynamic	μ_i	generalized Mean
W_e	Weissenberg number	δ_i	Generalized Variance
M	Mean Position	β	Adjustment Parameter

2. Mathematical formulation of drainage problem

In this section, mathematical formulation of non-Newtonian MHD Johnson Segalman fluid on outer surface of long vertical cylinder for drainage problem is briefly discussed [5].

2.1. Basic Equations

Basic equation governing the flow of incompressible fluid neglecting the thermal effects are given as

$$\nabla.\underline{V} = 0, \tag{1}$$

$$\rho \frac{D\mathbf{V}}{Dt} = \nabla.\boldsymbol{\sigma} + \rho\mathbf{f}, \tag{2}$$

where $\underline{V}$ is velocity vector of fluid, $\mathbf{f}$ is body force, $\frac{D}{Dt}$ is material time derivative, ρ denotes density ,Cauchy stress tensor is presented by σ and in case of Johnson Segalman fluid it is defined by [6]

$$\boldsymbol{\sigma} = \mathbf{T} - p\mathbf{I}, \tag{3}$$

$$\mathbf{T} = \mathbf{S} + 2\mu\mathbf{D}, \tag{4}$$

$$\mathbf{S} + m\left[\frac{D\mathbf{S}}{Dt} + \mathbf{S}(\mathbf{W} - a\mathbf{D}) + (\mathbf{W} - a\mathbf{D})^T\mathbf{S}\right] = 2\eta\mathbf{D}, \tag{5}$$

$$\frac{D\mathbf{S}}{Dt} = \frac{\partial\mathbf{S}}{\partial t} + (grad\mathbf{S})V, \tag{6}$$

in Eq (3) $-p\mathbf{I}$ is an intermediate part of stress due to incompressibility., a is slip parameter and viscosities are denoted by μ and η.

$$\mathbf{D} = \frac{1}{2}\left[\mathbf{L} + \mathbf{L}^T\right], \quad \mathbf{W} = \frac{1}{2}\left[\mathbf{L} - \mathbf{L}^T\right], \tag{7}$$

where $\mathbf{D}$ and $\mathbf{W}$ are symmetric and skew symmetric components of velocity gradient respectively. $\mathbf{L}$ which is defined as $grad\underline{\mathbf{V}}$. In case of $\eta = \mu = 0$ and $a = 1$, non-Newtonian Johnson Segalman fluid is transformed into newtonian model and Maxwell fluid respectively.

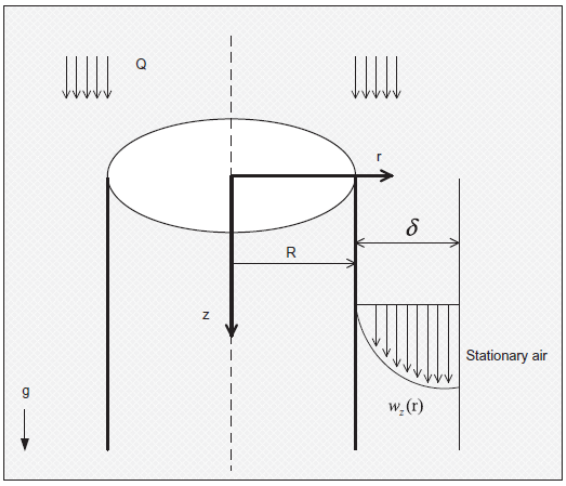

Figure 1. Schematic view of drainage problem [6]

2.2. Formulation

Vertically long cylinder of radius R is considered with non-Newtonian MHD Johnson–Segalman fluid on its outer surface as shown in Figure 1. Fluid is considered in the form of uniform axisymmetric thin film with thickness δ and in stationary contact with air. It is assumed that time has no effect on flow (steady state), surface tension is zero and pressure acting on fluid is atmospheric pressure so velocity profile $\underline{V}$ is given as

$$\underline{V} = [0, 0, w(r)]\,. \tag{8}$$

Radial direction is considered parpendicular to cylinder while z-axis is in downward direction horizontal to cylinder as prescribed in Figure 1. Boundary conditions for free space are given as

$$\text{at } r = R + \delta, \qquad T_{rz} = 0, \tag{9}$$

In case of no slip conditions, we have

$$\text{at } r = R, \qquad w = 0, \tag{10}$$

here T_{rz} denotes component of shear stress. Continuity equation Eq (1) is satisfied identically by using Eq (3) and Eq (4) thus Eq (2) is reduce to

$$0 = -\frac{\delta p}{\delta r} + \rho f_1, \tag{11}$$

$$0 = -\frac{1}{r}\frac{\partial p}{\partial \theta} + \rho f_2, \tag{12}$$

$$0 = -\frac{\partial p}{\partial z} + \frac{1}{r}\frac{d\,(rT_{rz})}{dr} + \rho f_3, \tag{13}$$

components of force in polar coordinates r,θ and z components are presented by f_1, f_2 and f_3 respectively. Since pressure is assumed to be constant and gravitational force is acting vertically downward therefore Eq (13) can is written as

$$0 = \frac{1}{r}\frac{d\,(rT_{xy})}{dr} + \rho g. \tag{14}$$

Non zero component of **S** is obtained by using Eq (6) and Eq (7) in Eq (5), we get

$$S_{rr} = \frac{(a-1)\eta m \left(\frac{dw}{dr}\right)^2}{1-(a^2-1)\, m^2 \left(\frac{dw}{dr}\right)^2}, \tag{15}$$

$$S_{rz} = S_{zr} = \frac{\eta \left(\frac{dw}{dr}\right)}{1+m^2\,(1-a^2)\left(\frac{dw}{dr}\right)^2}, \tag{16}$$

$$S_{zz} = \frac{\eta m(1+a)\left(\frac{dw}{dr}\right)^2}{1-(a^2-1)\, m^2 \left(\frac{dw}{dr}\right)^2}. \tag{17}$$

By using Eqs (15)-(17) in Eq (4) following components of Cauchy stress tensor **T** are obtained

$$T_{rr} = \frac{(a-1)\eta m \left(\frac{dw}{dr}\right)^2}{1-(a^2-1)\, m^2 \left(\frac{dw}{dr}\right)^2}, \tag{18}$$

$$T_{rz} = T_{zr} = \mu\left(\frac{dw}{dr}\right) + \frac{\eta \left(\frac{dv}{dr}\right)}{1-(a^2-1)\, m^2 \left(\frac{dw}{dr}\right)^2}, \tag{19}$$

$$T_{zz} = \frac{\eta m(1+a)\left(\frac{dw}{dr}\right)^2}{1+m^2\,(1-a^2)\left(\frac{dw}{dr}\right)^2}. \tag{20}$$

Now Eq (13) can be written as

$$\frac{d}{dr}\left[r\left(\mu\left(\frac{dw}{dr}\right) + \frac{\eta \left(\frac{dw}{dr}\right)}{1+m^2\,(1-a^2)\left(\frac{dw}{dr}\right)^2}\right)\right] = -\rho g r, \tag{21}$$

with boundary conditions

$$\text{at } r = R+\delta, \quad \frac{dw}{dr} = 0 \quad \text{(free surface)}\,, \tag{22}$$

$$\text{at } r = R, \quad w = 0 \quad \text{(no slip condition)}\,. \tag{23}$$

Now using similarity transformation by defining the following dimensionless parameters,

$$w^* = \frac{w}{U_0}, \quad r^* = \frac{r}{\delta}, \quad \delta^* = \frac{\delta}{R}, \quad T^*_{rz} = \frac{T_{rz}}{(\mu+\eta)\frac{U_0}{\delta}}, \quad \phi = \frac{\mu}{(\mu+\eta)}, \tag{24}$$

using equations in (24) and omitting $*$ in Eq (21) we have

$$\frac{d}{dr}\left[r\left(\phi\left(\frac{dw}{dr}\right) + \frac{(1-\phi)\left(\frac{dw}{dr}\right)}{1+W_e^2\,(1-a^2)\left(\frac{dw}{dr}\right)^2}\right)\right] = -rS_t, \tag{25}$$

with conditions

$$\text{at } r = R+\delta, \quad \frac{dw}{dr} = 0 \quad \text{(free surface)}\,, \tag{26}$$

$$\text{at } r = 1, \quad w = 0 \quad \text{(no slip condition)}, \tag{27}$$

where W_e and S_t are Weissenberg and Stokes numbers respectively and defined are as

$$W_e = \frac{mU_o}{\delta}, \qquad S_t = \frac{\rho g \delta^2}{\mu_{eff} U_0} \quad \text{and} \qquad \mu_{eff} = (\eta + \mu). \tag{28}$$

Integration of Eq (25) yields the drainage problem as under

$$\begin{aligned} &\frac{dw}{dr} + \phi W_e^2 \left(1 - a^2\right) \left(\frac{dw}{dr}\right)^3 - \frac{S_t}{2} W_e^2 \left(1 - a^2\right) \left((1+\delta)^2 \frac{1}{r} - r\right) \left(\frac{dw}{dr}\right)^2 \\ &\quad = \frac{S_t}{2} \left((1+\delta)^2 \frac{1}{r} - r\right), \qquad w(1) = 0, \end{aligned} \tag{29}$$

$w(r)$ denotes the velocity profile of Johnson Segalman fluid in radial direction.

3. The LNN-GNDO-SQP algorithm

The designed scheme consists of two major parts, first Legendre polynomials based artificial neural networks (LNN's) model is developed, and secondly, the neurons in LNN architecture for drainage problem are optimized by using hybridization of GNDO and SQP algorithms.

3.1. Series solution based on LNN structure

Mathematical model of approximate solution for drainage problem is developed by using LNN structure in terms of weighted legendre polynomials. Trial or approximate series solution $w(r)$ with first order derivative $w'(r)$ in terms of layers in LNN is mathematically expressed as

$$w(r) = \sum_{j=1}^{m} \alpha_j L_n \left(\omega_j r + \beta_j\right), \tag{30}$$

where α_i, ω_i and β_i are design weights and n shows the number of Legendre polynomials involved in Eq (30) and

$$\frac{dw}{dr}(r) = \sum_{j=1}^{m} \alpha_j \frac{dL_n}{dr} \left(\omega_j r + \beta_j\right), \tag{31}$$

where L_n denotes legendre polynomials. First three legendre polynomials are given as

$$L_1(r) = 1, \qquad L_2(r) = r, \qquad L_3(r) = \frac{1}{2}\left(3r^2 - 1\right), \qquad L_4(r) = \frac{1}{2}\left(5r^3 - 3r\right). \tag{32}$$

Higher order polynomials are generated by

$$L_{n+1}(r) = \frac{1}{n+1}\left[(2n+1) r L_n(r) - n L_{n-1}(r)\right]. \tag{33}$$

ANN structure for drainage problem in term of input, hidden and outer layer is shown in Figure 3.

3.2. Construction of fitness function

An objective function also known as fitness function or merit function is constructed based on mean square errors in candidate solutions to train unknown weights in LNN. Structure of fitness function is formulated as

$$\min \quad \varepsilon = \varepsilon_1 + \varepsilon_2, \tag{34}$$

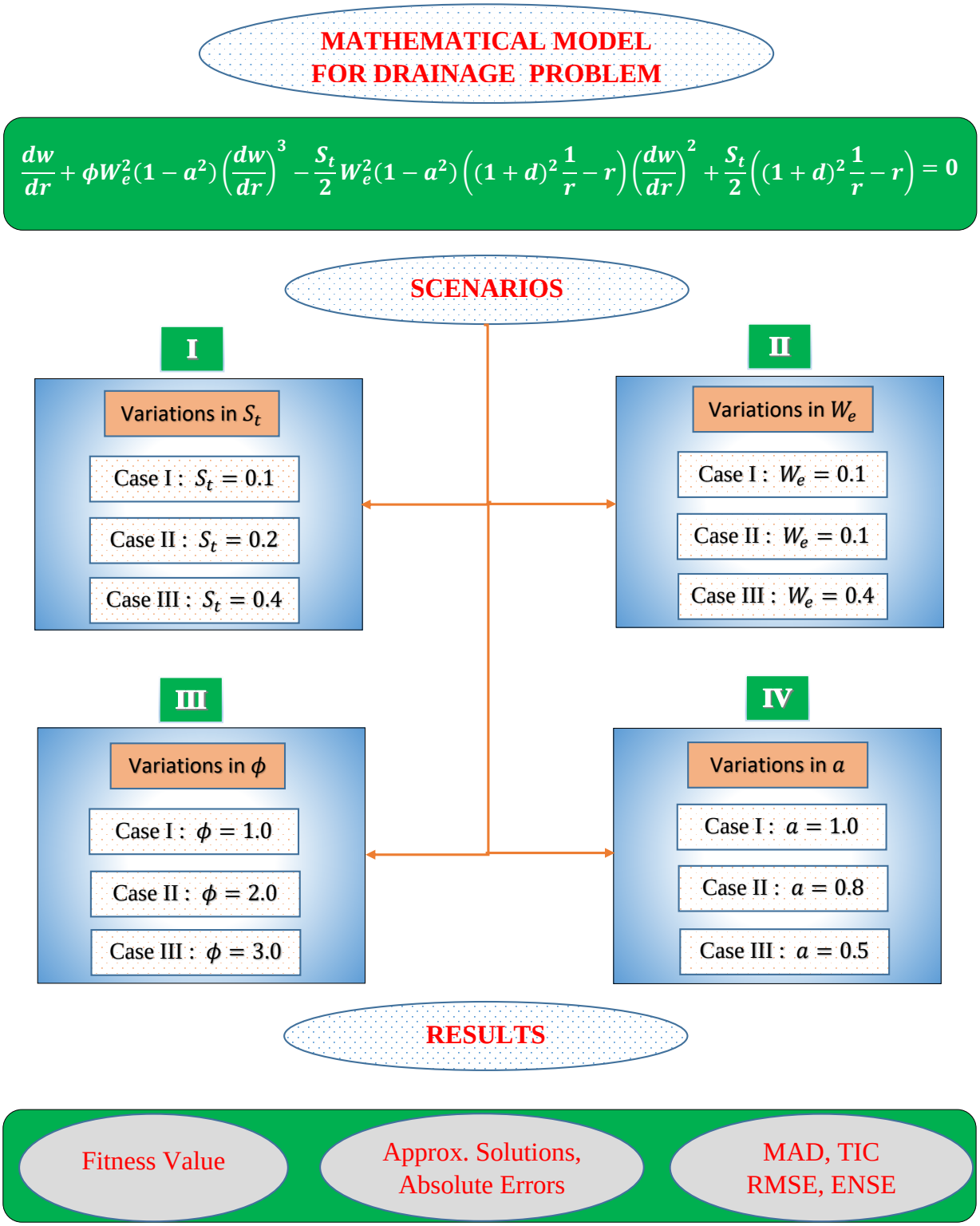

Figure 2. Graphical overview of the problem considered in this paper

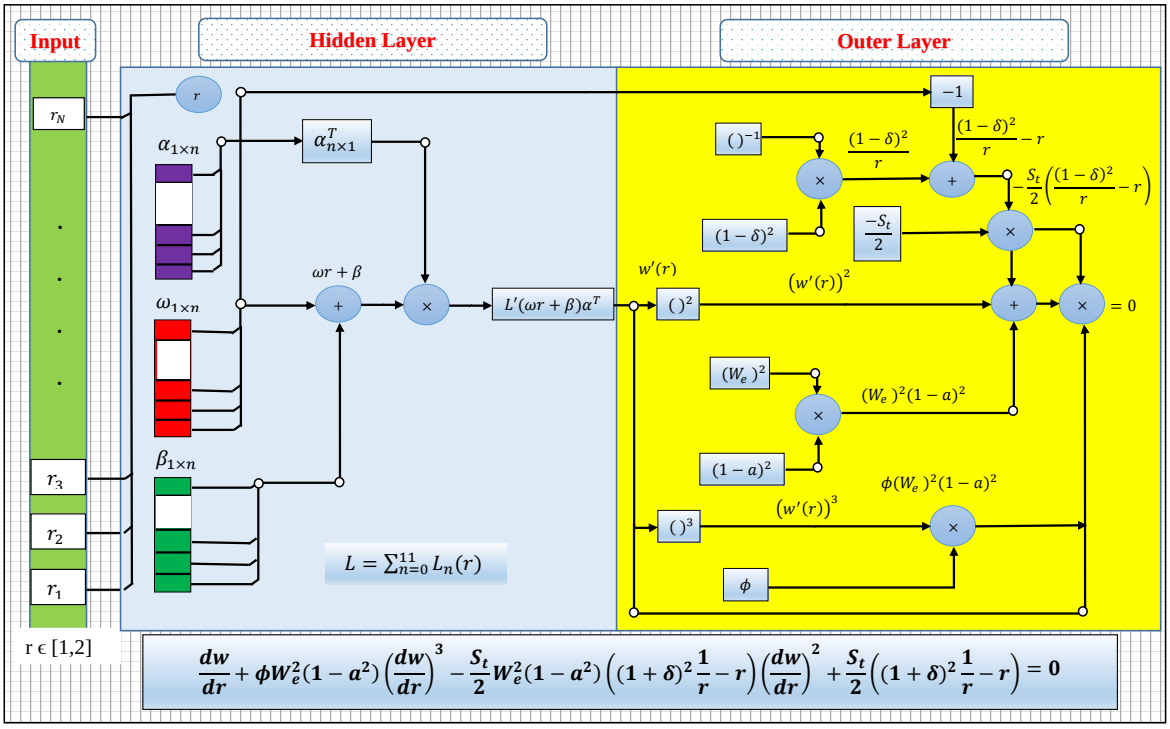

Figure 3. Legendre polynomial based artificial neural networks architecture for drainage problem.

ε_1 is mean square error in candidate solution by using it in drainage problem which is

$$\varepsilon_1=\frac{1}{n}\sum_{m=1}^{n}\left(\begin{array}{c}\frac{d\hat{w}_m}{dr}+\phi W_e^2\left(1-a^2\right)\left(\frac{d\hat{w}_m}{dr}\right)^3-\frac{S_t}{2}W_e^2\left(1-a^2\right)\\ \times\left((1+\delta)^2\frac{1}{r}-r\right)\left(\frac{d\hat{w}_m}{dr}\right)^2-\frac{S_t}{2}\left((1+\delta)^2\frac{1}{r}-r\right)\end{array}\right)^2, \tag{35}$$

where $N=\frac{1}{h}, \hat{w}_m=\hat{w}\left(r_m\right), r_m=mh$ ε_2 is the mean square error in candidate solution by putting it in initial condition, which is

$$\varepsilon_2=(w(1)-0)^2. \tag{36}$$

3.3. Optimization framework used to compute best weights

A novel methodology is adopted for calculating unknown weights in LNN by optimizing a fitness function see Eq (35), for drainage problem using a hybrid procedure of generalized normal distribution optimization (GNDO) technique and sequential quadratic programming (SQP). A detailed pseudo-code is given as Algorithm 1. An illustrative flowchart of the LNN-GNDO-SQP algorithm is given in Figure 4.

3.3.1. Brief introduction of generalized normal distribution optimization (GNDO) algorithm

The generalized normal distribution optimization technique is developed by Mirjalili [28], a novel metaheuristic algorithm inspired by normal distribution theory in which each individual's location is modified using a generalized normal curve for distribution. GNDO algorithm is an effective and efficient technique for finding optimal solutions for constrained and unconstrained optimization problems by enhancing and extracting the precision of unknown parameters. The working framework of the GNDO algorithm is classified into two main categories, named exploitation and exploration. The two phases are of equal importance in GNDO, and have the same probability of being chosen in

Algorithm 1: Pseudo-code for hybridized of the LNN-GNDO-SQP algorithm.

Global Search Phase
Generalized normal distribution optimizer: `Start`
Inputs: Population size N, The Upper and Lower bounds (u,l). Current number of iteration is t and maximum number of iterations is (Max_iter). Candidate solution with number of dimensions in each candidate solution are the set of unknown weights involved in ANN architecture, Weights = **C** $=[\alpha_i, \omega_i, \beta_i]$, $i = 1,2,3\ldots,n$.
Population: Generate population **P** of m candidates with the set of random weights drawn from a normal distribution as:
P=$[C_1,C_2,C_3,\ldots,C_m]^t$,
$\alpha=[\alpha_1,\alpha_2,\alpha_3,\ldots,\alpha_n]$, $\omega=[\omega_1,\omega_2,\omega_3,\ldots,\omega_n]$ and $\beta=[\beta_1,\beta_2,\beta_3,\ldots,\beta_n]$.
Output: Choose the current best solution i.e $C_{GNGO_{Best}}$.
Initializations: Initialize population **P**.
Fitness evaluation: Calculate the fitness value of each individual **C** in **P** and achieve the so far best solution x_{Best}.
The iteration is updated as $t = t+1$.
Main Loop
while $(t \leq (Max\_iter))$ **do**
for if $i = 1 : N$
p is randomly generated between 0 and 1.
if $p > 0.5$
Exploitation The current best solution x_{Best} is selected. **M**, δ, μ and η are calculated using Eqs (38)-(41) to perform exploitation.
else
Exploration The current best solution x_{Best} is selected an perform exploration using Eqs (42)-(44).
end if
end for
The iteration is updated as $t = t+1$.
end while
Termination: Stop GNDO if the following termination criteria meets
'Max_iter' reached
• Fitness $\epsilon \leq 10^{-20}$, TolFunc $\epsilon \leq 10^{-20}$
Storage: Store $C_{GNGO_{Best}}$, Fitness values and Function evaluations.
Generalized normal distribution Optimizer: End
Local Search Phase
Sequential Quadratic Programming: `Start`
Inputs: SQP starts with $C_{GNGO_{Best}}$ as its starting point
Output: GNDO-SQP best weights i.e., $C_{GNGO-SQP}$
Initialization: Start-Point as $C_{GNGO_{Best}}$ number of iterations, bound constraints.
Termination: Adaption process ends if any of the following conditions meet:
•Fitness $\epsilon = 10^{-18}$, total iterations $\leq$ 3000
•TolFun $\leq 10^{-18}$, TolX $\leq 10^{-20}$
•TolCon $\leq 10^{-18}$, MaxFunEvals $\leq$ to 200,000
while (satisfied the required termination)
Fitness evaluation: Calculate fitness of each weight vector **C**.
Fine-tuning: Use 'fmincon' for SQP. Update parameters of **C** for each generation of SQP and calculate fitness of modified **C**.
Storage: Accumulate weights vector $C_{GNDO-SQP}$, fitness value, iterations and functions evaluations.
Sequential quadratic programming: End
Data Generations: Repeat 100 times GNDO-SQP steps to obtain massive data set of the optimization variables of LNN to solve non-linear mathematical model of drainage problem.

Table 1. Parameter settings for GNDO and SQP algorithms.

Parameter	Setting	Parameter	Setting
Algorithm	GNDO	Bounds [lower, upper]	[-1,1]
Maximum Iterations	6000	X-tolerance (TolX)	10^{-20}
Maximum function evaluations	150,000	Search Agents	70
Fitness	10^{-20}	Function tolerance (TolFun)	10^{-20}
Algorithm	SQP	Bounds [lower, upper]	[-1,1]
Maximum Iterations	3000	Function tolerance (TolFun)	10^{-18}
Maximum function evaluations	200,000	X-tolerance (TolX)	10^{-20}

order to optimize a problem.

a) Exploitation : It is a process of finding optimum solutions around the candidate space containing the current position of individuals. This phase's working procedure is based on a relation between the normal distribution of population and the distribution of each individual in a population. The model for optimization can be expressed as

$$u_i^t = \delta_i \times \eta + \mu_i, \qquad i = 1, 2, 3, \ldots, N, \tag{37}$$

where δ_i, η and μ_i are defined as

$$\delta_i = \sqrt{\frac{1}{3}\left[\left(x_i^t - \mu\right)^2 + (\boldsymbol{M} - \mu)^2 + \left(x_{Best}^t - \mu\right)^2\right]}, \tag{38}$$

$$\eta = \begin{cases} \sqrt{-\log(\lambda_1)} \times \cos(2\pi\lambda_2), \text{ if } a <= b, \\ \sqrt{-\log(\lambda_1)} \times \cos(2\pi\lambda_2 + \pi), \text{ otherwise,} \end{cases} \tag{39}$$

$$\mu_i = \frac{1}{3}\left(x_i^t + x_{Best}^t + M\right), \tag{40}$$

u^t, μ_i and δ_i are trial vector, generalized mean and generalized variance of ith individual at any time t. Penalty factor is denoted by η. a, b, λ_1 and λ_2 are randomly chosen numbers between 0 and 1. x_{Best}^t which is the so far best position of individual while its mean position is denoted by M and defined as

$$\boldsymbol{M} = \frac{\sum_{i=1}^{N} \boldsymbol{x}_i^t}{N}. \tag{41}$$

b) Exploration : It is a process of searching a population space globally to find promising solutions. Global search phase in GNDO is subjected to three arbitrarily selected individuals, which are modeled as:

$$\boldsymbol{u}_i^t = \boldsymbol{x}_i^t + \beta \times (|\lambda_3| \times \boldsymbol{u}_1) + (1 - \beta) \times (|\lambda_4| \times \boldsymbol{u}_2), \tag{42}$$

local information is presented by $\boldsymbol{x}_i^t + \beta \times (|\lambda_3| \times \boldsymbol{v}_1)$ while global information is shared by $(1 - \beta) \times (|\lambda_4| \times \boldsymbol{v}_2)$. u_1 and u_2 are trail vectors while β is adjustment parameter between 0 and 1. u_1 and u_2 can be calculated as

$$\boldsymbol{u}_1 = \begin{cases} \boldsymbol{x}_i^t - \boldsymbol{x}_{\mathrm{pl}}^t, \text{ if } f\left(\boldsymbol{x}_i^t\right) < f\left(\boldsymbol{x}_{\mathrm{p1}}^t\right), \\ \boldsymbol{x}_{\mathrm{p1}}^t - \boldsymbol{x}_i^t, \text{ otherwise}, \end{cases} \tag{43}$$

and

$$\boldsymbol{u}_2 = \begin{cases} \boldsymbol{x}_{\mathrm{p2}}^t - \boldsymbol{x}_{\mathrm{p3}}^t, \text{ if } f\left(\boldsymbol{x}_{\mathrm{p2}}^t\right) < f\left(\boldsymbol{x}_{\mathrm{p3}}^t\right), \\ \boldsymbol{x}_{\mathrm{p3}}^t - \boldsymbol{x}_{\mathrm{p2}}^t, \text{ otherwise}, \end{cases} \tag{44}$$

where $p1 \neq p2 \neq p3 \neq i$ are integers between 1 to N.

3.3.2. Sequential Quadratic Programming

To enhance the local search characteristic of our solution technique, we have combined SQP with GNDO. SQP is a well-established single path following the local search algorithm, which has considerably enhanced our algorithm's convergence speed. SQP is considered a classical method developed in 1963 for solving constrained/unconstrained linear and nonlinear optimization problems [29]. The SQP algorithm is known to be one of the basic approaches to be used in the context of public and commercial sector problems of significant importance. Some recent applications of SQP includes numerical simulation of shakedown analysis of structure [30], economic load dispatch problem [31] and turbulent flow [32].

3.4. Hybridization of GNDO-SQP Algorithm

Working procedure of LNN-GNDO-SQP algorithm is summarized as :
Step 1 Initialization : Trial solution Eq (30) for drainage problem is considered and unknown parameters of LNN are initialized with randomly generated real values for population space. Mathematically, individuals can be listed as

$$C = [(\alpha, \omega, \beta)] = [\alpha_1, \alpha_2, \ldots \alpha_n, \omega_1, \omega_2, \ldots \omega_n, \beta_1, \beta_2, \ldots \beta_n], \tag{45}$$

where n denotes the number of weights in LNN model. Parameter setting for GNDO algorithm is given in Table 1.
Step 2 Fitness calculation : GNDO evaluate the fitness function Eq (35) and update the weights when required until termination criteria is achieved.
Step 3 Ranking : Unknown parameters attained with GNDO for error based function (fitness function) during multiple runs are ranked in ascending order.
Step 4 Initializing SQP : The unknown parameters corresponding to minimum value of fitness function achieved by GNDO are considered as the initial guess or initial weights to supervise sequential quadratic programming.
Step 5 Fitness calculation : Fitness function for drainage problem is calculated by using SQP algorithm with updated weights of GNDO.
Step 6 Stopping criteria : The weights are updated with GNDO-SQP algorithm and the process is stopped when minimum criteria on fitness value is achieved. Parameter settings for SQP is given in Table 1.
Step 7 Storage : Weights, fitness value, residual and absolute errors are stored for the optimization of drainage problem. Graphical overview of the LNN-GNDO-SQP algorithm given in Figure 4.

4. Statistical Evaluation

In this section, statistical analysis for different drainage problems based on mean, standard deviation and minimum values is presented. Performance indications like Mean absolute deviation (MAD), Theil's inequality coefficient (TIC), Root mean square error (RMSE), and Error in Nash Sutcliffe efficiency (ENSE) are defined to study the efficiency of the proposed algorithm. Global performance indicators like GMAD, GTIC, GRMSE, and GENSE are also defined to study our novel computing approach's overall performance. Formulation of performance metrics are given as

$$MAD = \frac{1}{n} \sum_{i=1}^{n} \left(\left| w\left(r_i\right) - w_{approx}\left(r_i\right) \right| \right), \tag{46}$$

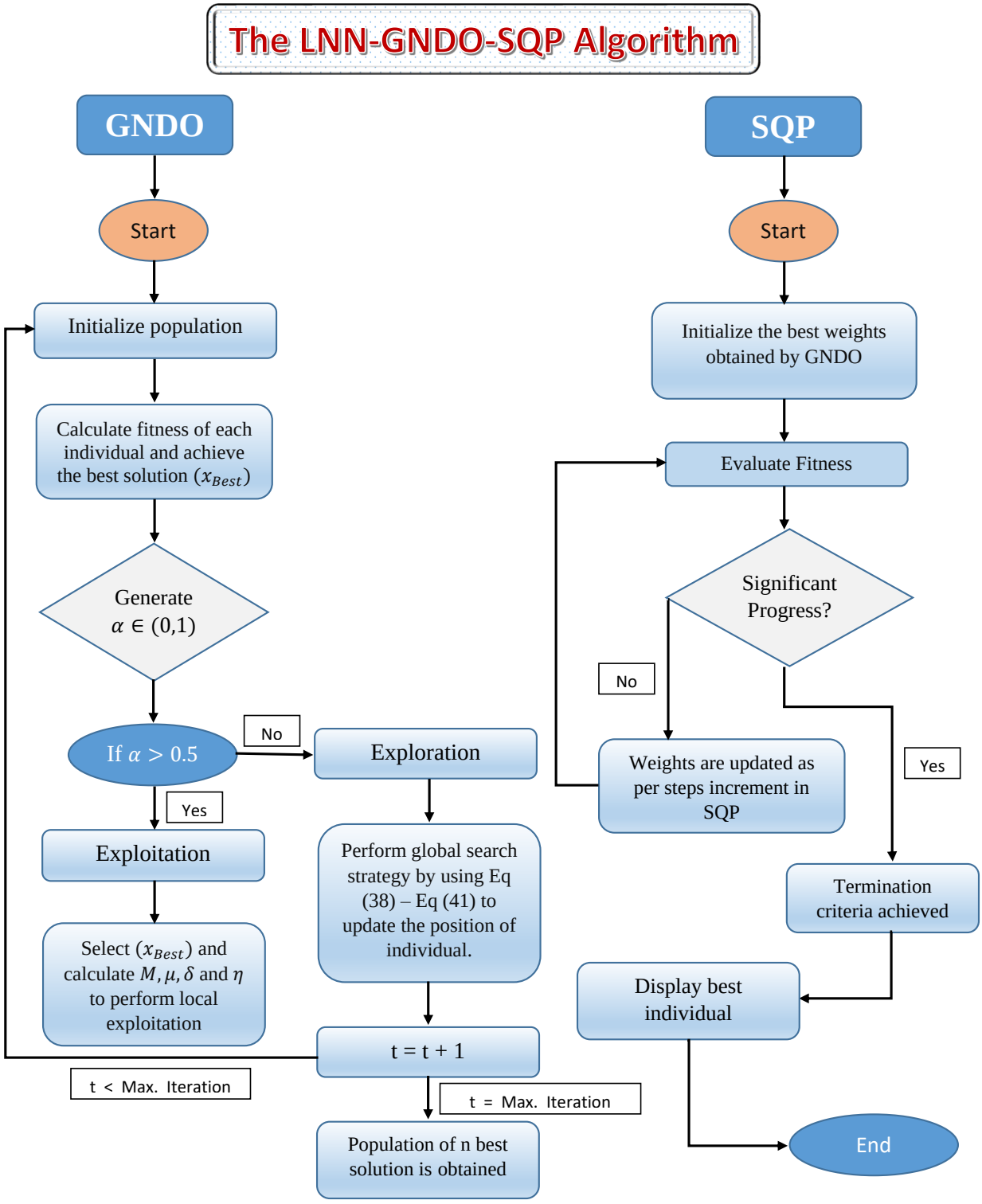

Figure 4. Flow chart of the LNN-GNDO-SQP Algorithm

$$TIC = \frac{\sqrt{\frac{1}{n}\sum_{i=1}^{n}\left(w\left(r_i\right)-w_{approx}\left(r_i\right)\right)^2}}{\sqrt{\frac{1}{n}\sum_{i=1}^{n}\left(w\left(r_i\right)\right)^2}+\sqrt{\frac{1}{n}\sum_{i=1}^{n}\left(w_{approx}\left(r_i\right)\right)^2}}, \tag{47}$$

$$RMSE = \frac{1}{n}\sqrt{\sum_{i=1}^{n}\left(w\left(r_i\right)-w_{approx}\left(r_i\right)\right)^2}, \tag{48}$$

$$\text{NSE} = \left\{1-\frac{\sum_{i=1}^{n}\left(w\left(r_i\right)-w_{approx}\left(r_i\right)\right)^2}{\sum_{i=1}^{n}\left(w\left(r_i\right)-\bar{w}\left(r_i\right)\right)^2}\right., \qquad \bar{w}\left(r_i\right)=\sum_{i=1}^{n}\left(w\left(r_i\right)\right), \tag{49}$$

$$ENSE = |1-NSE|, \tag{50}$$

here $\hat{w}(r_i) = w_{approx}(r_i)$.
In case of perfect solution, values of these performance indices must approaches to zero. Formulation of global performance indices are given as

$$GMAD = \frac{1}{R_n}\sum_{j=1}^{R_n} MAD, \quad GTIC = \frac{1}{R_n}\sum_{j=1}^{R_n} TIC, \quad GRMSE = \frac{1}{R_n}\sum_{j=1}^{R_n} RMSE, \quad GENSE = \frac{1}{R_n}\sum_{j=1}^{R_n} ENSE, \tag{51}$$

where R_n denotes the number of independent runs.

5. Numerical Experimentation

In this section different scenarios of non-linear drainage problem is considered with different cases depending on the variations in parameters like S_t, W_e, ϕ and a.
SCENARIO I: Effect of variation in Strokes number S_t on drainage problem. Following three cases are considered **CASE I** : $S_t = 0.1$, **CASE II** : $S_t = 0.3$ and **CASE III** : $S_t = 0.4$ where $W_e = \phi = 1$, $a = 0.1$ and thickness $\delta = 1$.
Fitness function Eq (35) for the scenario I is formulated as

$$\varepsilon = \frac{1}{n}\sum_{m=1}^{n}\left(\frac{d\hat{w}_m}{dr}+0.99\left(\frac{d\hat{w}_m}{dr}\right)^3-0.495S_t\left(\frac{4}{r}-r\right)\left(\frac{d\hat{w}_m}{dr}\right)^2-\frac{S_t}{2}\left(\frac{4}{r}-r\right)\right)^2+(w(1))^2. \tag{52}$$

SCENARIO II: Effect of variation in Weissenberg number W_e on drainage problem. Following three cases are considered **CASE I** : $W_e = 0.0$, **CASE II** : $W_e = 1.0$ and **CASE III** : $W_e = 2.0$ where $S_t = 0.5$, $\phi = 0.80$, $a = 0.50$ and thickness $\delta = 1.0$.
Fitness function Eq (35) for the scenario II is formulated as

$$\varepsilon = \frac{1}{n}\sum_{m=1}^{n}\left(\frac{d\hat{w}_m}{dr}+0.6W_e^2\left(\frac{d\hat{w}_m}{dr}\right)^3-0.1875W_e^2\left(\frac{4}{r}-r\right)\left(\frac{d\hat{w}_m}{dr}\right)^2-0.25\left(\frac{4}{r}-r\right)\right)^2+(w(1))^2. \tag{53}$$

SCENARIO III: Effect of variation in ratio of viscosities ϕ on drainage problem. Following three cases are considered **CASE I** : $\phi = 1.0$, **CASE II** : $\phi = 2.0$ and **CASE III** : $\phi = 3.0$ where $S_t = 0.5$, $W_e = 1.0$, $a = 0.50$ and thickness $\delta = 1.0$.
Fitness function Eq (35) for the scenario III is formulated as

$$\varepsilon = \frac{1}{n}\sum_{m=1}^{N}\left(\frac{d\hat{w}_m}{dr}+0.75\phi\left(\frac{d\hat{w}_m}{dr}\right)^3-0.1875\left(\frac{4}{r}-r\right)\left(\frac{d\hat{w}_m}{dr}\right)^2-0.25\left(\frac{4}{r}-r\right)\right)^2+(w(1))^2. \tag{54}$$

SCENARIO IV: Effect of variation in slip parameter a on drainage problem. Following three cases are considered **CASE I** : $a = 1.0$, **CASE II** : $a = 0.8$ and **CASE III** : $a = 0.5$ where $S_t = 0.70$, $W_e = 1.30$,

$\phi = 0.60$ and thickness $\delta = 1.0$.
Fitness function Eq (35) for the scenario IV is formulated as

$$\varepsilon_1 = \frac{1}{n}\sum_{m=1}^{n}\left(\frac{d\hat{w}_m}{dr} + 1.014\left(1-a^2\right)\left(\frac{d\hat{w}_m}{dr}\right)^3 - 0.5915\left(1-a^2\right)\left(\frac{4}{r}-r\right)\left(\frac{d\hat{w}_m}{dr}\right)^2 - 0.35\left(\frac{4}{r}-r\right)\right)^2 + (w(1))^2 . \tag{55}$$

6. Results and Discussion

In this paper, the mathematical model MHD thin film flow of non Newtonian fluid is formulated for drainage. Four scenarios are considered depending on the variations in parameters, including Stokes number S_t, Weissenberg number W_e, a ratio of viscosities ϕ, and slip parameter a. A novel soft computing technique is developed to solve the non-linear mathematical model for drainage problem, see Eq (29). Approximate solutions obtained by our proposed technique, the LNN-GNDO-SQP algorithm, are compared with MATLAB solver RK-4 and hybrid of genetic algorithm and active set algorithm (GA-ASA) [33].
Fitness functions as in Eq (52)-Eq (55) corresponding to four scenarios of drainage problem are optimized by performing 100 independent runs using the LNN-GNDO-SQP algorithm. It is evident from Figure 5 that best approximated solutions obtained by proposed scheme overlaps the numerical and GA-ASA solutions for each scenario. Furthermore, it can be seen from Figure 5(a) and 5(b) that with increase in stokes and Weissenberg number the velocity profile $w(r)$ of Johnson Segalman fluid increases while from Figure 5(c) and 5(d) it is observed that $w(r)$ decreases with increase in ratio of viscosity and slip parameters. The unknown weights involved in calculation of best solutions are visualized in Figure 7. Graphical illustration for performance of the designed algorithm in obtaining change in velocity profile and absolute errors in best solutions for all scenarios are shown in Figure 6 and 8. Convergence of fitness values for each scenario with different cases are shown in Figure 9. Approximate solution and absolute errors in best solution for each scenario are listed in Tables 2-5. Absolute errors (AE) in scenario I lies around 10^{-13} to 10^{-15}, 10^{-11} to 10^{-13} and 10^{-12} to 10^{-15}. AE in scenario II lies around 10^{-11} to 10^{-13}, 10^{-10} to 10^{-14} and 10^{-9} to 10^{-12}. AE in scenario III lies around 10^{-11} to 10^{-13}, 10^{-12} to 10^{-14} and 10^{-12} to 10^{-15}. AE in scenario IV lies around 10^{-10} to 10^{-14}, 10^{-11} to 10^{-16} and 10^{-9} to 10^{-11}. It is obvious from these errors that our approach is successful in calculating best solutions with less errors. Weights obtained by proposed scheme for optimization of fitness functions $(Eq(52) - Eq(55))$ are given in Tables 6-9. These weights are useful in producing our results.
The comparison of statistical data for absolute errors in term of minimum, mean, and standard deviation for scenario I, II, III, and IV obtained by the LNN-GNDO-SQP algorithm are compared with GA-ASA [33] as shown in Tables 10-13. It can be seen that minimum values, mean and standard deviation at each step size $r = 0.05$ dominates the techniques available in the latest literature [33]. Statistical data of MAD, TIC, RMSE, and ENSE in terms of minimum, mean and standard deviation are presented in Tables 14-17. Minimum values of fitness, MAD, TIC, RMSE and ENSE for different cases of each scenarios lies around 10^{-11} to 10^{-12}, 10^{-6} to 10^{-7}, 10^{-6} to 10^{-7} and 10^{-9} to 10^{-11} respectively. In Figures 10, 11, 12 and 15 normal probability curves for performance indicators are presented. Bar graphs are plotted to illustrate values of the global performance indicators MAD, TIC, RMSE, and ENSE. Global values of performance indices lie between 10^{-6} and 10^{-7}, which establishes our algorithm's superiority.

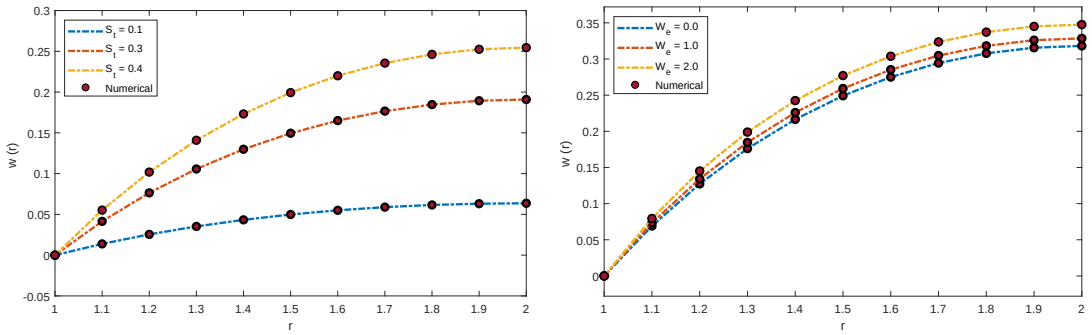

(a) SCENARIO I **(b)** SCENARIO II

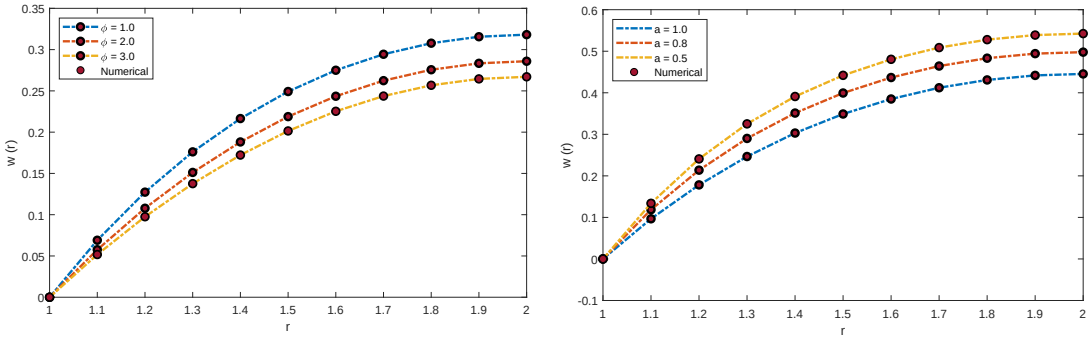

(c) SCENARIO III **(d)** SCENARIO IV

Figure 5. Comparison of dimensionless velocity profile obtained by LNN-GNDO-SQP algorithm with RK-4 method for variants of drainage problem.

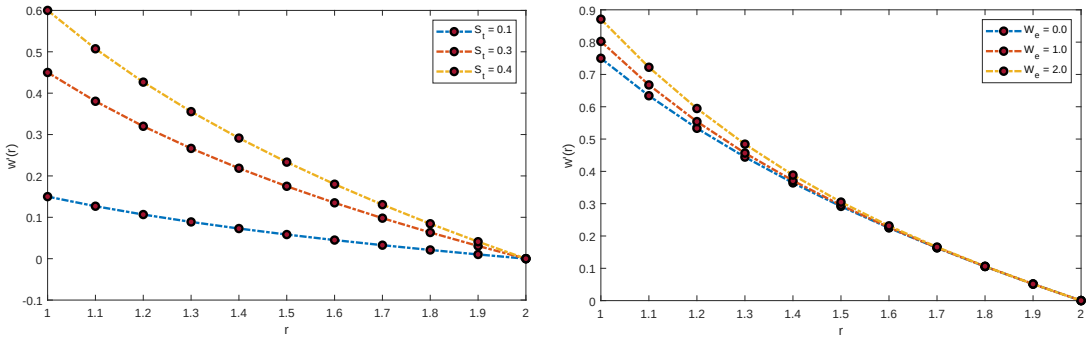

(a) SCENARIO I **(b)** SCENARIO II

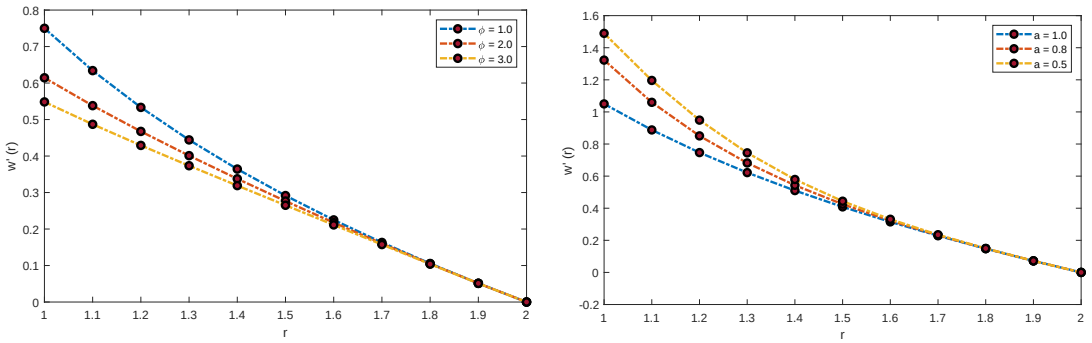

(c) SCENARIO III **(d)** SCENARIO IV

Figure 6. Comparison of values obtained for w' by our proposed algorithm. Influence of variations in S_t, W_e, ϕ and a is studied for mathematical model of drainage problem.

Table 2. Approximate solutions and Absolute errors obtained by LNN-GNDO-SQP algorithm for SCENARIO I of drainage problem.

	Solutions			Absolute Errors		
r	Case I	Case II	Case III	Case I	Case II	Case III
1.0	-1.17E-09	-2.93E-08	6.62E-10	7.36E-15	1.46E-13	7.92E-15
1.1	0.013812	0.041437	0.055248	2.22E-13	4.19E-12	3.18E-13
1.2	0.025464	0.076393	0.101857	9.24E-13	1.15E-11	1.77E-12
1.3	0.035223	0.105669	0.140892	5.42E-13	6.59E-13	1.59E-12
1.4	0.043295	0.129884	0.173178	7.71E-14	6.31E-12	3.22E-14
1.5	0.049843	0.149529	0.199372	5.64E-13	1.99E-13	1.35E-12
1.6	0.055001	0.165002	0.220003	8.59E-16	5.31E-12	5.64E-14
1.7	0.058876	0.176627	0.235503	5.17E-13	3.23E-14	1.08E-12
1.8	0.061557	0.184672	0.246230	4.41E-13	5.84E-12	1.15E-12
1.9	0.063121	0.189363	0.252483	6.69E-14	3.74E-12	1.88E-13
2.0	0.063630	0.190888	0.254518	1.44E-15	1.53E-13	3.73E-15

Table 3. Approximate solutions and Absolute errors obtained by LNN-GNDO-SQP algorithm for SCENARIO II of drainage problem.

	Solutions			Absolute Errors		
r	Case I	Case II	Case III	Case I	Case II	Case III
1.0	1.60E-08	3.22E-07	-3.79E-08	1.36E-12	4.02E-12	8.29E-12
1.1	0.069061	0.073286	0.079469	3.16E-11	9.00E-11	3.04E-10
1.2	0.127322	0.134214	0.145147	4.85E-11	1.19E-10	1.22E-09
1.3	0.176115	0.184630	0.198951	1.53E-12	1.37E-12	2.25E-10
1.4	0.216473	0.225933	0.242478	2.22E-11	5.98E-11	6.80E-10
1.5	0.249216	0.259191	0.277061	8.46E-13	4.37E-12	1.33E-10
1.6	0.275004	0.285236	0.303803	1.49E-11	3.50E-11	7.24E-10
1.7	0.294379	0.304720	0.323602	1.64E-13	6.82E-12	4.98E-11
1.8	0.307788	0.318167	0.337161	8.70E-12	3.03E-11	8.39E-10
1.9	0.315605	0.325992	0.345010	3.80E-12	2.07E-12	5.67E-10
2.0	0.318148	0.328535	0.347552	4.01E-13	4.65E-14	3.25E-11

Table 4. Approximate solutions and Absolute errors obtained by LNN-GNDO-SQP algorithm for SCENARIO III of drainage problem.

	Solutions			Absolute Errors		
r	Case I	Case II	Case III	Case I	Case II	Case III
1.0	2.78E-08	1.20E-09	2.25E-08	4.35E-13	2.14E-14	4.41E-14
1.1	0.069061	0.057570	0.051729	7.19E-12	9.73E-13	5.33E-13
1.2	0.127322	0.107809	0.097514	2.55E-11	4.13E-12	1.59E-12
1.3	0.176115	0.151207	0.137633	3.95E-12	1.41E-12	1.12E-12
1.4	0.216473	0.188122	0.172252	1.03E-11	1.40E-12	1.25E-13
1.5	0.249216	0.218821	0.201457	2.40E-12	1.01E-12	9.50E-13
1.6	0.275004	0.243515	0.225278	8.30E-12	9.73E-13	3.04E-14
1.7	0.294379	0.262388	0.243717	1.39E-12	7.36E-13	9.64E-13
1.8	0.307787	0.275618	0.256782	8.39E-12	5.05E-13	4.97E-13
1.9	0.315604	0.283396	0.264522	4.71E-12	6.68E-13	3.53E-14
2.0	0.318148	0.285937	0.267060	3.78E-13	6.83E-14	2.76E-15

Table 5. Approximate solutions and Absolute errors obtained by LNN-GNDO-SQP algorithm for SCENARIO IV of drainage problem.

	Solutions			Absolute Errors		
r	Case I	Case II	Case III	Case I	Case II	Case III
1.0	-3.30E-08	1.39E-07	8.89E-06	6.40E-12	9.89E-15	8.73E-11
1.1	0.096686	0.118626	0.133905	1.22E-10	5.24E-12	1.43E-09
1.2	0.178252	0.213761	0.240778	2.32E-10	1.91E-11	2.21E-08
1.3	0.246561	0.290113	0.325136	1.23E-12	6.64E-12	1.35E-08
1.4	0.303063	0.351164	0.391060	1.40E-10	4.51E-13	1.18E-09
1.5	0.348903	0.399427	0.441979	2.86E-14	2.21E-12	7.60E-09
1.6	0.385007	0.436712	0.480563	1.20E-10	6.22E-14	3.52E-11
1.7	0.412130	0.464339	0.508748	3.26E-13	2.41E-16	7.55E-09
1.8	0.430903	0.483280	0.527879	1.47E-10	6.13E-13	2.46E-10
1.9	0.441847	0.494259	0.538894	7.02E-11	7.23E-13	1.05E-10
2.0	0.445406	0.497823	0.542465	3.18E-12	3.27E-14	6.17E-10

Table 6. Best set of weights obtained by the LNN-GNDO-SQP algorithm using fitness function as in Eq (52). Here three cases are studied by varying S_t in the drainage problem.

	Case I			Case II			Case III		
index	α_j	ω_j	β_j	α_j	ω_j	β_j	α_j	ω_j	β_j
1	-0.267240	-0.002610	0.304056	-0.161130	0.245666	0.153137	-0.642690	-0.817430	0.856846
2	0.199856	0.083281	0.361633	0.540048	-0.082950	-0.133580	-0.500960	-0.085350	0.282074
3	0.574441	-0.211200	-0.000280	0.999999	0.004495	0.031383	-0.502540	-0.411400	0.346607
4	0.939992	0.009259	-0.304090	-0.609000	-0.206300	-0.187450	0.986752	-0.145940	0.599804
5	-0.411700	0.102550	0.009940	-0.952670	-0.488120	0.153461	0.627584	0.615380	-0.986650
6	-0.280860	0.091810	-0.271960	0.042458	0.321851	-0.117770	0.271924	-0.325700	-0.085320
7	0.172679	-0.600230	0.705329	-0.101030	-0.283540	0.999321	0.243758	0.265845	-0.090110
8	0.065151	0.313916	0.079046	-0.277050	0.204757	0.353785	-0.863580	-0.368860	0.070886
9	0.159743	-0.031440	0.179555	0.373401	-0.330670	0.288077	-0.155260	-0.116030	-0.412520
10	0.433358	-0.300480	0.174122	0.363993	0.240191	0.020892	0.825776	-0.133910	0.119581
11	-0.362530	-0.225430	0.133951	0.999719	0.041990	0.288770	-0.148830	-0.229960	-0.050250

Table 7. Best set of weights obtained by the LNN-GNDO-SQP algorithm using fitness function as in Eq (53). Here three cases are studied by varying W_e in the drainage problem.

	Case I			Case II			Case III		
index	α_j	ω_j	β_j	α_j	ω_j	β_j	α_j	ω_j	β_j
1	-0.277180	-0.928610	0.990229	-0.984680	-0.867220	0.370173	-0.575380	-0.988420	0.997400
2	-0.744240	0.990077	-0.999960	-0.801200	0.555550	-0.024790	-0.999990	0.131423	0.343622
3	-0.553260	-0.988500	0.923460	-0.002580	0.129594	-0.998370	0.143249	-0.854240	0.140163
4	-0.404730	0.398152	0.127399	-0.047010	0.700149	-0.999990	-0.119360	0.373826	0.207802
5	-0.809510	0.036150	0.140306	-0.690450	0.398839	-0.196860	-0.856660	-0.352810	0.010636
6	0.698433	0.464628	0.151832	0.301364	0.237875	0.160810	-0.797780	-0.322780	0.999999
7	-0.003180	0.192692	0.395066	0.423747	0.272096	-0.176540	-0.645030	-0.182700	-0.655790
8	-0.150320	-0.098370	-0.558090	-0.997780	-0.212630	-0.417770	0.012084	0.257723	-0.149790
9	-0.992840	-0.329570	0.734408	0.274115	-0.255500	0.001304	-0.753090	-0.306120	0.466878
10	0.182691	-0.066350	-0.374700	-0.428760	-0.199540	0.929899	0.498251	0.125154	0.236910
11	-0.629380	-0.361980	0.101130	-0.138360	-0.138270	0.103016	0.079987	0.174965	0.126845

Table 8. Best set of weights obtained by the LNN-GNDO-SQP algorithm using fitness function as in Eq (54). Here three cases are studied by varying ϕ in the drainage problem.

	Case I			Case II			Case III		
index	α_j	ω_j	β_j	α_j	ω_j	β_j	α_j	ω_j	β_j
1	-0.578170	0.090627	0.621742	-0.719570	0.999994	-0.664540	-0.841870	0.915168	-0.247580
2	0.642790	-0.552250	0.999977	0.863347	-0.300220	0.348017	0.456016	0.271674	0.687734
3	-0.984330	0.465779	-0.162840	-0.759410	-0.863760	0.994778	0.408307	-0.370890	0.016365
4	-0.620110	0.128942	0.566053	-0.413700	0.378054	0.137548	0.125005	-0.162090	-0.313500
5	0.924819	-0.630340	0.993488	-0.284960	-0.285900	0.692566	-0.316870	0.173333	0.750680
6	-0.282300	0.331916	0.220188	-0.354880	-0.672930	-0.554160	-0.118880	0.196454	-0.250040
7	0.999998	-0.258550	-0.093070	-0.000860	0.398419	-0.803340	0.886842	0.542877	-0.637760
8	-0.934180	0.280345	-0.632150	0.218599	-0.235300	-0.046750	-0.225580	-0.157780	-0.417790
9	-0.179500	-0.705000	0.207103	-0.460840	-0.145630	0.673652	0.425031	0.174465	0.278200
10	0.000931	0.269963	0.264995	-0.163930	0.280319	-0.353570	-0.998280	-0.306190	0.186654
11	0.367440	0.270983	-0.105050	0.161173	0.188646	-0.083490	-0.547840	0.271897	0.005882

Table 9. Best set of weights obtained by the LNN-GNDO-SQP algorithm using fitness function as in Eq (55). Here three cases are studied by varying a in the drainage problem.

	Case I			Case II			Case IIi		
index	α_j	ω_j	β_j	α_j	ω_j	β_j	α_j	ω_j	β_j
1	-0.937800	0.260055	-0.599770	-0.996410	0.505919	-0.254550	-1.357140	1.301247	-1.342750
2	0.373960	-0.384460	-0.286000	0.308871	0.389527	0.441955	1.620159	-0.810600	-0.543930
3	0.862114	0.210662	-0.163780	0.841584	0.082865	0.640732	0.153404	-1.187130	-0.400690
4	-0.996400	0.758110	-0.974980	0.992297	-0.456590	-0.13996	0.025061	0.244749	0.341770
5	-0.616540	-0.416200	0.113885	-0.844170	0.661252	-0.369140	-1.162260	-0.289160	-0.150160
6	-0.729390	0.223456	0.069204	0.348376	-0.289810	0.556567	-1.254670	-0.224680	-0.178620
7	0.810262	0.262491	-0.492080	-0.999670	-0.061340	-0.055630	1.221794	0.082876	0.282458
8	0.885861	-0.200570	-0.356040	0.256956	-0.775240	0.414591	0.300091	0.123791	0.165290
9	0.690933	0.109413	0.407307	0.054504	-0.465980	-0.080880	-1.119120	0.256081	0.135531
10	-0.702680	-0.316270	0.484328	0.289438	-0.128410	0.146051	0.830104	0.241196	0.291386
11	-0.080280	-0.212490	0.046098	-0.616560	0.295517	-1.000000	-1.171850	-0.266330	-0.063730

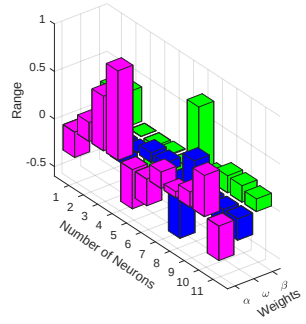

(a) $S_t = 0.1$

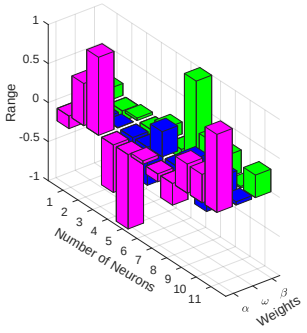

(b) $S_t = 0.3$

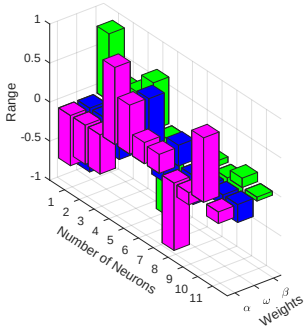

(c) $S_t = 0.4$

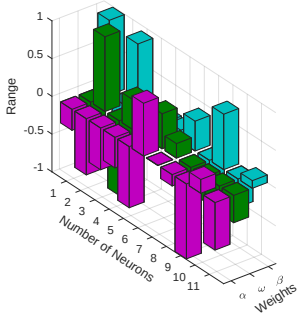

(d) $W_e = 0.0$

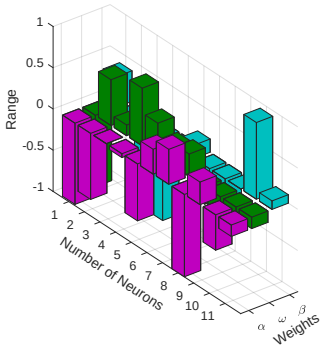

(e) $W_e = 1.0$

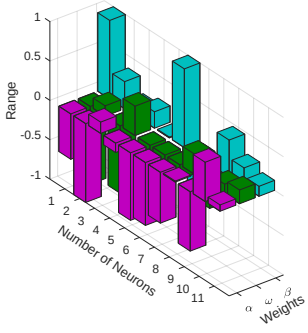

(f) $W_e = 2.0$

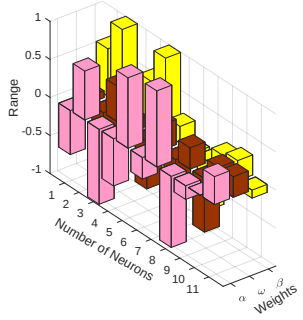

(g) $\phi = 1.0$

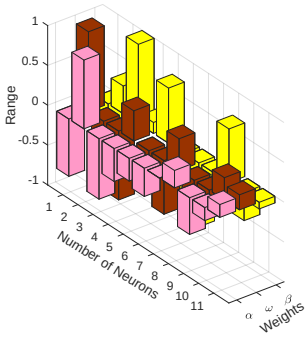

(h) $\phi = 2.0$

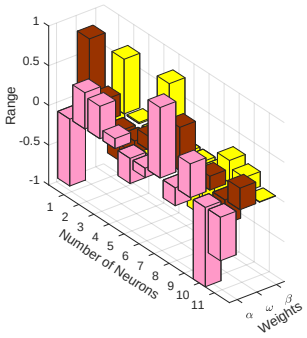

(i) $\phi = 3.0$

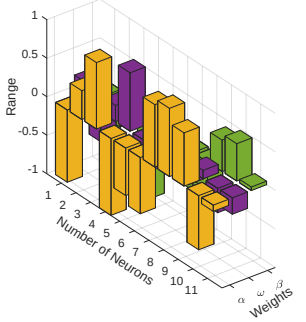

(j) $a = 1.0$

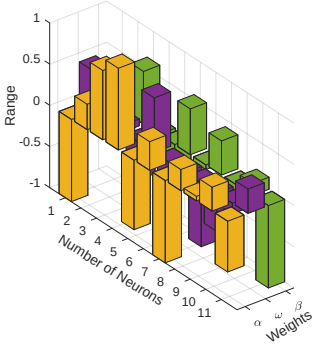

(k) $a = 2.0$

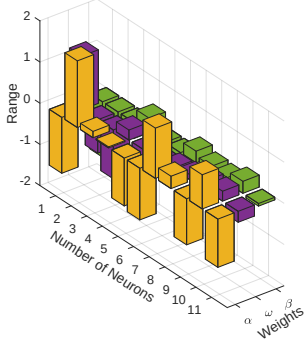

(l) $a = 3.0$

Figure 7. Plots of weights used in calculating best solutio for scenarios I, II, III and IV.

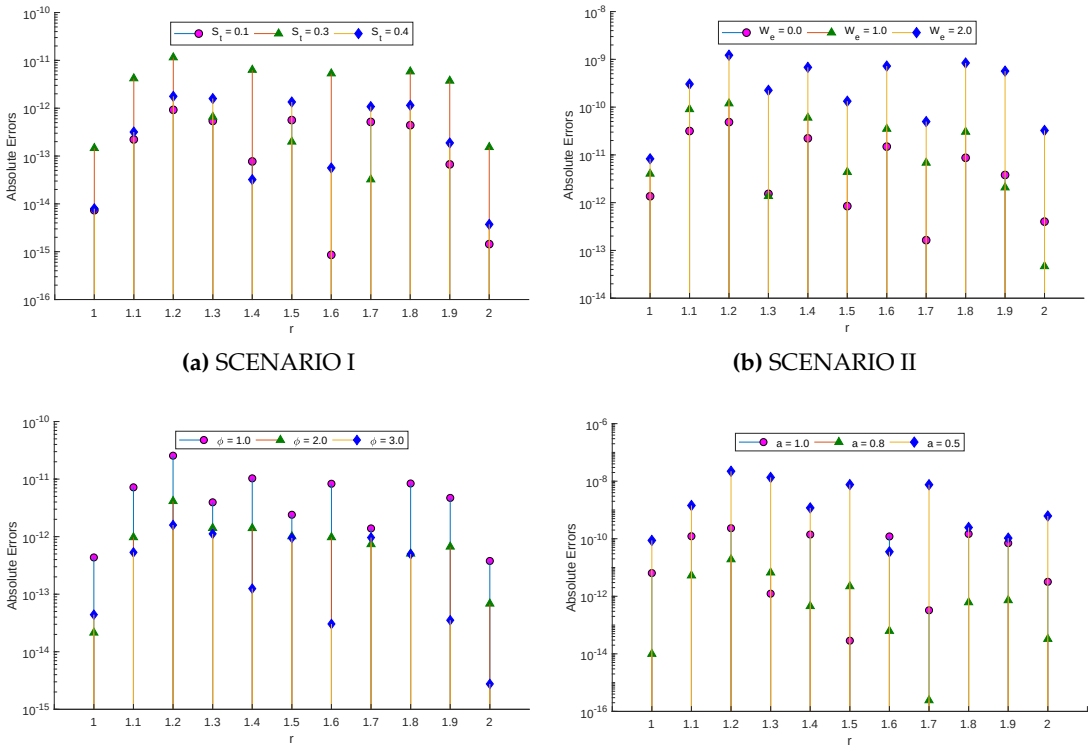

(a) SCENARIO I **(b)** SCENARIO II

(c) SCENARIO III **(d)** SCENARIO IV

Figure 8. Absolute errors in solutions calculated by LNN-GNDO-SQP algorithm solutions for scenarios of drainage problem.

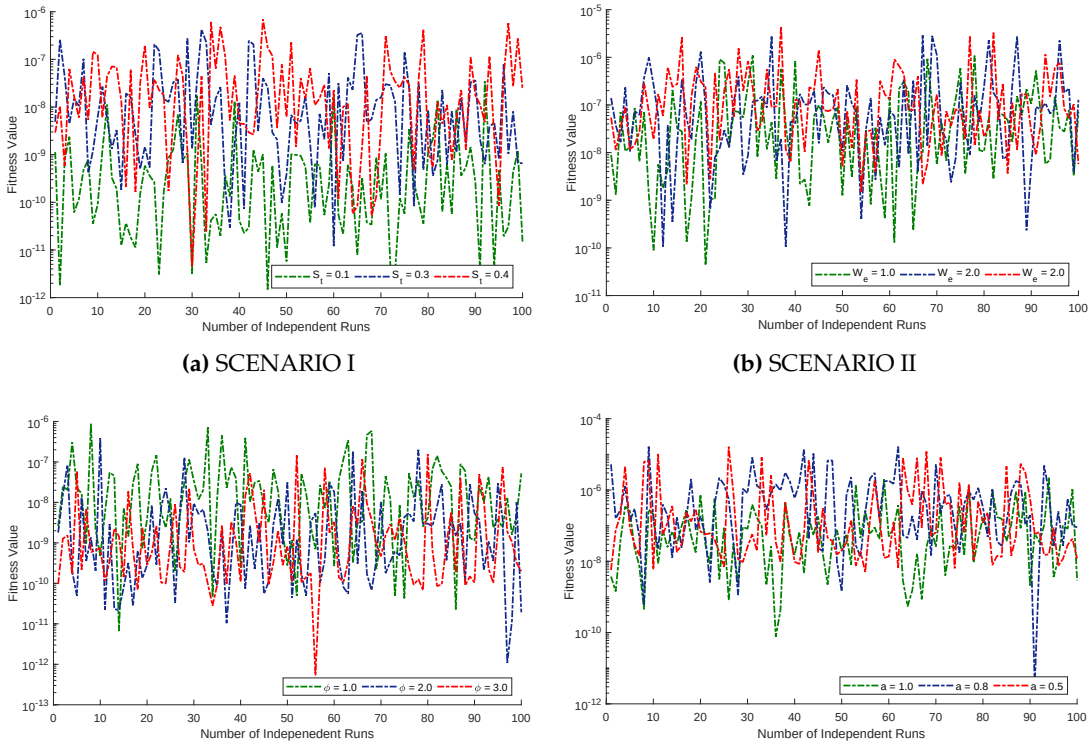

(a) SCENARIO I **(b)** SCENARIO II

(c) SCENARIO III **(d)** SCENARIO IV

Figure 9. Fitness values obtained by LNN-GNDO-SQP algorithm, for four scenarios of drainage problem during 100 runs.

Table 10. Statistical analysis of the results obtained by the LNN-GNDO-SQP algorithm, GA-ASA technique on the 21 steps within the interval [1 2], It is evident that LNN-GNDO-SQP is superior in accuracy and stability. Three cases of drainage problem are considered based on variations in S_t.

	Case I						Case II						Case III					
	Min		Mean		Std		Min		Mean		Std		Min		Mean		Std	
	GA-ASA	GNDO-SQP	GA-ASA	GNDO-SQP	GA-ASA	GNDO-SQP	GA-ASA	GNDO-SQP	GA-ASA	GNDO-SQP	GA-ASA	GNDO-SQP	GA-ASA	GNDO-SQP	GA-ASA	GNDO-SQP	GA-ASA	GNDO-SQP
1	5.7E-13	**7.36E-15**	5.0E-09	**7.72E-10**	3.8E-08	**2.73E-09**	4.0E-12	**1.46E-13**	1.3E-07	1.90E-08	5.7E-07	**5.22E-08**	1.9E-12	**7.92E-15**	2.7E-07	**2.58E-08**	8.4E-07	**7.13E-08**
1.05	1.1E-08	**5.74E-12**	1.2E-06	**2.01E-09**	7.6E-07	**4.24E-09**	6.8E-08	**5.04E-11**	2.4E-06	**5.48E-08**	1.5E-06	**8.88E-08**	2.0E-09	**2.36E-11**	1.8E-06	**1.08E-07**	1.4E-06	**1.65E-07**
1.1	1.6E-08	**2.22E-13**	3.8E-06	**2.76E-09**	2.6E-06	**8.25E-09**	1.7E-07	**4.19E-12**	6.6E-06	**7.09E-08**	3.9E-06	**1.60E-07**	1.0E-07	**3.18E-13**	4.9E-06	**1.14E-07**	4.0E-06	**2.52E-07**
1.15	3.0E-08	**5.15E-15**	5.5E-06	**1.19E-09**	3.9E-06	**4.56E-09**	1.7E-07	**2.08E-17**	9.0E-06	**2.88E-08**	5.4E-06	**8.43E-08**	1.2E-08	**2.75E-14**	6.4E-06	**3.53E-08**	5.6E-06	**1.15E-07**
1.2	1.0E-08	**9.24E-13**	5.7E-06	**2.52E-10**	4.4E-06	**5.98E-10**	1.1E-07	**7.62E-16**	8.7E-06	**6.22E-09**	5.5E-06	**1.04E-08**	2.9E-09	**1.77E-12**	5.9E-06	**1.04E-08**	5.6E-06	**1.13E-08**
1.25	2.1E-08	**2.96E-16**	4.7E-06	**4.58E-10**	4.0E-06	**5.55E-10**	5.5E-08	**2.20E-13**	6.5E-06	**1.23E-08**	4.3E-06	**1.47E-08**	1.1E-09	**6.32E-14**	4.1E-06	**2.91E-08**	4.1E-06	**3.52E-08**
1.3	4.5E-08	**2.74E-17**	3.1E-06	**9.68E-10**	3.2E-06	**2.47E-09**	2.4E-08	**6.00E-16**	3.6E-06	**2.43E-08**	2.6E-06	**4.66E-08**	1.2E-08	**5.12E-13**	2.0E-06	**4.42E-08**	2.1E-06	**8.52E-08**
1.35	2.8E-09	**1.27E-13**	1.6E-06	**1.13E-09**	2.2E-06	**3.96E-09**	1.7E-09	**1.15E-14**	1.1E-06	**2.69E-08**	1.4E-06	**7.11E-08**	1.3E-08	**1.29E-12**	8.0E-07	**3.97E-08**	1.1E-06	**1.17E-07**
1.4	6.9E-10	**1.46E-14**	7.1E-07	**8.67E-10**	1.4E-06	**3.39E-09**	5.7E-09	**8.39E-13**	1.2E-06	**2.01E-08**	1.1E-06	**5.99E-08**	1.3E-08	**3.22E-14**	1.6E-06	**2.57E-08**	1.4E-06	**8.77E-08**
1.45	1.4E-08	**1.57E-13**	6.4E-07	**4.80E-10**	8.0E-07	**1.50E-09**	8.3E-09	**1.73E-12**	1.4E-06	**1.13E-08**	1.4E-06	**2.61E-08**	4.1E-08	**3.36E-15**	1.7E-06	**1.65E-08**	1.5E-06	**3.38E-08**
1.5	2.2E-09	**2.32E-17**	6.4E-07	**2.58E-10**	9.0E-07	**3.57E-10**	1.2E-09	**3.64E-15**	1.0E-06	**6.80E-09**	1.8E-06	**9.65E-09**	8.4E-09	**4.54E-14**	1.3E-06	**1.52E-08**	1.5E-06	**2.22E-08**
1.55	3.8E-08	**3.18E-13**	1.8E-06	**3.25E-10**	1.4E-06	**4.87E-10**	1.3E-07	**3.50E-12**	3.2E-06	**8.48E-09**	2.3E-06	**1.14E-08**	3.3E-08	**2.49E-13**	2.7E-06	**1.75E-08**	2.0E-06	**2.40E-08**
1.6	5.6E-08	**1.10E-16**	3.2E-06	**5.95E-10**	2.2E-06	**1.98E-09**	6.6E-08	**4.75E-14**	5.9E-06	**1.38E-08**	3.6E-06	**3.38E-08**	3.1E-08	**5.64E-14**	4.7E-06	**2.14E-08**	3.8E-06	**5.59E-08**
1.65	1.9E-08	**4.89E-14**	4.5E-06	**8.48E-10**	3.2E-06	**3.19E-09**	6.3E-08	**2.24E-12**	8.2E-06	**1.87E-08**	5.2E-06	**5.42E-08**	1.6E-10	**1.05E-12**	6.3E-06	**2.50E-08**	5.8E-06	**8.37E-08**
1.7	1.1E-07	**5.40E-16**	5.3E-06	**8.23E-10**	3.9E-06	**2.71E-09**	3.3E-09	**1.42E-17**	9.6E-06	**1.84E-08**	6.3E-06	**4.62E-08**	1.6E-08	**2.83E-16**	7.2E-06	**2.65E-08**	7.0E-06	**6.74E-08**
1.75	1.6E-07	**3.07E-14**	5.5E-06	**4.88E-10**	4.0E-06	**1.05E-09**	1.3E-08	**2.94E-12**	9.7E-06	**1.21E-08**	6.5E-06	**1.92E-08**	2.4E-09	**1.92E-14**	7.2E-06	**2.14E-08**	7.2E-06	**3.10E-08**
1.8	3.0E-08	**7.97E-14**	5.0E-06	**1.65E-10**	3.6E-06	**2.47E-10**	3.6E-09	**5.84E-12**	8.3E-06	**4.86E-09**	5.6E-06	**7.95E-09**	9.1E-08	**7.91E-13**	6.0E-06	**1.07E-08**	6.0E-06	**1.66E-08**
1.85	2.8E-08	**1.28E-14**	3.8E-06	**4.91E-10**	3.1E-06	**1.74E-09**	1.9E-09	**1.06E-13**	5.7E-06	**1.01E-08**	3.8E-06	**2.84E-08**	3.9E-09	**1.81E-14**	3.9E-06	**1.44E-08**	3.9E-06	**4.67E-08**
1.9	4.7E-08	**6.64E-14**	2.4E-06	**1.45E-09**	3.1E-06	**4.59E-09**	7.2E-08	**2.93E-12**	2.7E-06	**3.12E-08**	2.0E-06	**7.28E-08**	3.8E-09	**1.88E-13**	1.9E-06	**4.69E-08**	1.6E-06	**1.13E-07**
1.95	3.1E-08	**1.31E-12**	1.4E-06	**1.33E-09**	3.3E-06	**3.11E-09**	2.8E-09	**1.73E-11**	1.3E-06	**3.14E-08**	2.0E-06	**5.16E-08**	1.3E-08	**2.77E-12**	1.7E-06	**5.29E-08**	1.8E-06	**8.46E-08**
2	3.5E-08	**1.44E-15**	1.3E-06	**2.64E-10**	2.7E-06	**9.19E-10**	2.8E-09	**7.27E-14**	1.2E-06	**5.42E-09**	2.1E-06	**1.43E-08**	2.1E-08	**3.73E-15**	1.6E-06	**7.45E-09**	1.9E-06	**2.13E-08**

Table 11. Statistical analysis of the results obtained by the LNN-GNDO-SQP algorithm, GA-ASA technique on the 21 steps within the interval [1 2], It is evident that LNN-GNDO-SQP is superior in accuracy and stability. Three cases of drainage problem are considered based on variations in W_e.

	Case I						Case II						Case III					
	Min		Mean		Std		Min		Mean		Std		Min		Mean		Std	
	GA-ASA	GNDO-SQP	GA-ASA	GNDO-SQP	GA-ASA	GNDO-SQP	GA-ASA	GNDO-SQP	GA-ASA	GNDO-SQP	GA-ASA	GNDO-SQP	GA-ASA	GNDO-SQP	GA-ASA	GNDO-SQP	GA-ASA	GNDO-SQP
1	4.4E-12	**1.30E-12**	4.5E-07	**5.90E-08**	1.2E-06	**1.56E-07**	2.5E-12	**1.13E-12**	2.5E-07	**1.26E-07**	5.5E-07	**3.84E-07**	4.4E-11	**3.95E-12**	8.9E-07	**7.34E-08**	1.5E-06	**2.14E-07**
1.05	5.0E-08	**2.50E-10**	2.3E-06	**1.48E-07**	1.9E-06	**2.05E-07**	2.4E-08	**3.97E-10**	2.2E-06	**4.00E-07**	2.1E-06	**6.79E-07**	3.8E-08	**5.99E-09**	3.7E-06	**8.42E-07**	2.2E-06	**1.35E-06**
1.1	5.3E-09	**3.10E-11**	6.2E-06	**2.02E-07**	5.2E-06	**4.20E-07**	4.1E-08	**3.79E-11**	5.8E-06	**4.88E-07**	5.6E-06	**1.19E-06**	1.9E-08	**3.04E-10**	9.1E-06	**5.35E-07**	5.6E-06	**1.27E-06**
1.15	7.6E-08	**6.50E-13**	8.5E-06	**8.54E-08**	7.5E-06	**2.55E-07**	1.2E-08	**4.07E-15**	7.5E-06	**1.88E-07**	7.5E-06	**6.32E-07**	9.4E-08	**6.61E-11**	1.0E-05	**8.18E-08**	7.0E-06	**2.91E-07**
1..20	5.1E-08	**3.91E-11**	8.3E-06	**2.17E-08**	7.8E-06	**4.26E-08**	1.1E-08	**1.16E-11**	6.8E-06	**4.62E-08**	7.3E-06	**7.96E-08**	1.7E-08	**1.22E-09**	7.5E-06	**9.24E-08**	5.8E-06	**1.06E-07**
1.25	6.1E-08	**1.37E-11**	6.3E-06	**3.91E-08**	6.5E-06	**4.60E-08**	3.2E-09	**1.33E-17**	4.7E-06	**9.64E-08**	5.3E-06	**1.24E-07**	1.0E-08	**2.58E-13**	3.3E-06	**2.17E-07**	3.1E-06	**3.39E-07**
1.3	9.7E-08	**4.14E-14**	3.9E-06	**7.06E-08**	4.1E-06	**1.13E-07**	2.4E-09	**1.33E-12**	2.4E-06	**1.72E-07**	2.7E-06	**3.47E-07**	4.2E-09	**3.43E-11**	1.7E-06	**2.32E-07**	2.2E-06	**5.68E-07**
1.35	1.1E-08	**3.54E-13**	1.9E-06	**7.42E-08**	2.1E-06	**1.93E-07**	3.7E-09	**8.98E-13**	9.9E-07	**1.80E-07**	1.2E-06	**5.34E-07**	1.4E-09	**1.66E-13**	3.5E-06	**1.60E-07**	3.3E-06	**5.34E-07**
1.4	3.6E-09	**4.24E-14**	1.2E-06	**5.56E-08**	1.6E-06	**1.81E-07**	2.0E-08	**4.79E-12**	1.8E-06	**1.32E-07**	1.9E-06	**4.62E-07**	2.1E-07	**6.73E-10**	4.0E-06	**8.92E-08**	2.8E-06	**2.92E-07**
1.45	2.2E-08	**5.61E-12**	1.6E-06	**3.67E-08**	1.8E-06	**8.83E-08**	7.4E-09	**2.32E-11**	2.2E-06	**8.11E-08**	2.3E-06	**2.10E-07**	6.8E-08	**8.44E-11**	3.5E-06	**6.14E-08**	2.0E-06	**8.49E-08**
1.5	5.8E-08	**1.84E-15**	2.0E-06	**2.85E-08**	1.9E-06	**3.49E-08**	2.9E-09	**9.44E-14**	2.0E-06	**5.78E-08**	2.8E-06	**8.39E-08**	1.1E-07	**1.37E-14**	5.4E-06	**6.91E-08**	2.9E-06	**1.10E-07**
1.55	2.2E-08	**1.50E-12**	3.5E-06	**2.99E-08**	2.7E-06	**3.91E-08**	2.5E-08	**7.70E-12**	3.5E-06	**6.45E-08**	3.5E-06	**9.95E-08**	9.0E-08	**2.37E-11**	9.2E-06	**9.04E-08**	4.6E-06	**1.72E-07**
1.6	1.7E-07	**8.41E-13**	5.5E-06	**3.71E-08**	4.5E-06	**8.48E-08**	2.6E-08	**9.82E-14**	5.5E-06	**9.02E-08**	5.5E-06	**2.42E-07**	1.3E-07	**7.69E-13**	1.2E-05	**1.10E-07**	7.4E-06	**3.51E-07**
1.65	2.3E-07	**2.66E-14**	7.4E-06	**4.80E-08**	6.6E-06	**1.55E-07**	5.7E-09	**5.69E-15**	7.1E-06	**1.19E-07**	7.8E-06	**4.09E-07**	8.7E-08	**1.96E-10**	1.3E-05	**1.20E-07**	9.8E-06	**4.26E-07**
1.7	4.8E-08	**5.72E-15**	8.5E-06	**5.51E-08**	8.1E-06	**1.41E-07**	7.8E-11	**1.30E-13**	7.9E-06	**1.28E-07**	9.3E-06	**3.63E-07**	6.1E-08	**2.39E-13**	1.2E-05	**1.09E-07**	1.1E-05	**2.97E-07**
1.75	7.2E-08	**1.76E-14**	8.6E-06	**4.50E-08**	8.4E-06	**6.36E-08**	7.2E-10	**4.60E-12**	7.9E-06	**9.46E-08**	9.3E-06	**1.60E-07**	5.2E-08	**2.64E-11**	1.0E-05	**7.30E-08**	9.9E-06	**1.24E-07**
1.8	1.6E-08	**8.70E-12**	7.5E-06	**2.07E-08**	7.4E-06	**3.09E-08**	1.7E-08	**4.33E-12**	6.7E-06	**4.12E-08**	7.7E-06	**7.66E-08**	9.3E-08	**2.03E-11**	7.5E-06	**4.04E-08**	7.4E-06	**7.10E-08**
1.85	1.6E-07	**7.63E-15**	5.4E-06	**2.51E-08**	5.3E-06	**7.82E-08**	1.8E-08	**4.60E-13**	4.6E-06	**6.22E-08**	4.9E-06	**2.10E-07**	3.2E-08	**4.38E-14**	4.7E-06	**8.19E-08**	4.4E-06	**2.93E-07**
1.9	2.0E-08	**2.25E-13**	3.1E-06	**9.39E-08**	2.8E-06	**2.20E-07**	7.4E-09	**2.07E-12**	2.3E-06	**2.15E-07**	2.3E-06	**5.72E-07**	1.1E-08	**6.58E-11**	3.4E-06	**2.13E-07**	2.7E-06	**6.23E-07**
1.95	2.7E-08	**9.58E-12**	2.1E-06	**1.12E-07**	2.1E-06	**1.68E-07**	4.2E-08	**6.95E-12**	2.3E-06	**2.39E-07**	2.7E-06	**4.37E-07**	1.0E-07	**7.58E-11**	4.5E-06	**2.03E-07**	3.4E-06	**4.18E-07**
2	1.2E-07	**2.11E-13**	2.3E-06	**1.43E-08**	2.1E-06	**4.03E-08**	2.3E-08	**4.65E-14**	2.2E-06	**3.37E-08**	2.7E-06	**1.05E-07**	2.1E-08	**4.91E-12**	4.6E-06	**4.08E-08**	3.2E-06	**1.38E-07**

Table 12. Statistical analysis of the results obtained by the LNN-GNDO-SQP algorithm, GA-ASA technique on the 21 steps within the interval [1 2], It is evident that LNN-GNDO-SQP is superior in accuracy and stability. Three cases of drainage problem are considered based on variations in ϕ.

	Case I						Case II						Case III					
	Min		Mean		Std		Min		Mean		Std		Min		Mean		Std	
	GA-ASA	GNDO-SQP	GA-ASA	GNDO-SQP	GA-ASA	GNDO-SQP	GA-ASA	GNDO-SQP	GA-ASA	GNDO-SQP	GA-ASA	GNDO-SQP	GA-ASA	GNDO-SQP	GA-ASA	GNDO-SQP	GA-ASA	GNDO-SQP
1	2.2E-13	3.88E-13	6.9E- 07	**4.89E-08**	1.5E-06	**1.43E-07**	2.4E-11	**2.14E-14**	1.2E-06	**9.21E-09**	2.3E-06	**3.82E-08**	2.5E-11	5.70E-16	1.4E-06	5.98E-09	3.6E-06	1.97E-08
1.05	6.3E-09	**1.41E-10**	1.1E-06	**2.07E-07**	1.6E-06	**3.33E-07**	9.8E-09	**3.13E-12**	2.0E-06	**5.14E-08**	2.6E-06	**1.27E-07**	1.1E-08	**2.41E-11**	2.1E-06	**3.34E-08**	3.5E-06	6.93E-08
1.1	8.8E-09	**7.19E-12**	1.9E-06	**2.23E-07**	2.2E-06	**5.21E-07**	1.2E-07	**9.73E-13**	4.1E-06	**4.85E-08**	3.8E-06	**1.75E-07**	2.0E-07	**5.33E-13**	3.3E-06	**3.14E-08**	4.4E-06	**8.86E-08**
1.15	1.5E-08	**3.90E-17**	1.9E-06	**7.30E-08**	2.3E-06	**2.42E-07**	3.2E-07	**2.44E-15**	4.7E-06	**1.35E-08**	4.6E-06	**6.70E-08**	9.7E-09	**2.68E-12**	3.7E-06	**8.43E-09**	5.4E-06	**2.95E-08**
1..20	3.4E-08	**2.55E-11**	1.3E-06	**2.01E-08**	1.8E-06	**2.36E-08**	1.6E-07	**6.37E-13**	3.6E-06	**5.07E-09**	4.3E-06	**6.59E-09**	4.8E-08	**1.59E-12**	3.1E-06	**2.68E-09**	5.3E-06	**3.97E-09**
1.25	1.3E-09	**1.15E-14**	8.1E-07	**5.28E-08**	1.3E-06	**6.37E-08**	1.5E-08	**1.51E-13**	1.9E-06	**1.39E-08**	3.4E-06	**2.64E-08**	6.2E-09	**1.45E-14**	2.2E-06	**8.82E-09**	4.2E-06	**1.71E-08**
1.3	1.5E-09	**8.10E-14**	1.0E-06	**8.50E-08**	1.6E-06	**1.76E-07**	1.2E-08	**3.76E-13**	1.9E-06	2.00E-08	2.7E-06	**6.99E-08**	2.2E-08	**1.04E-13**	1.6E-06	**1.37E-08**	3.2E-06	3.96E-08
1.35	1.2E-08	**1.06E-13**	1.3E-06	**8.11E-08**	1.8E-06	**2.42E-07**	4.5E-08	**2.18E-13**	2.9E-06	1.78E-08	2.5E-06	**8.30E-08**	3.4E-11	**9.58E-14**	1.9E-06	**1.26E-08**	3.5E-06	4.20E-08
1.4	5.7E-08	**4.22E-12**	1.4E-06	**5.58E-08**	1.7E-06	**1.88E-07**	8.6E-08	**3.89E-13**	2.9E-06	**1.16E-08**	2.5E-06	**5.50E-08**	5.5E-08	**1.25E-13**	2.8E-06	**7.72E-09**	4.0E-06	**2.42E-08**
1.45	9.9E-09	**9.32E-13**	1.7E-06	**3.39E-08**	2.1E-06	**7.25E-08**	1.9E-08	**1.06E-15**	2.9E-06	**6.78E-09**	2.6E-06	**1.69E-08**	4.4E-08	**2.42E-13**	3.3E-06	**3.20E-09**	3.7E-06	**5.96E-09**
1.5	8.3E-09	**1.90E-14**	2.8E-06	**2.67E-08**	3.3E-06	**3.87E-08**	2.2E-07	**1.14E-14**	5.3E-06	**5.59E-09**	3.8E-06	**9.79E-09**	2.0E-07	**1.28E-14**	3.5E-06	**2.14E-09**	3.2E-06	**4.36E-09**
1.55	1.2E-08	**9.34E-12**	3.8E-06	**3.24E-08**	4.9E-06	**4.50E-08**	4.3E-08	**4.68E-15**	8.1E-06	**7.61E-09**	6.3E-06	**1.83E-08**	5.8E-08	**2.58E-14**	4.0E-06	**4.91E-09**	4.6E-06	**1.28E-08**
1.6	5.1E-09	**1.21E-13**	4.3E-06	**4.48E-08**	6.2E-06	**1.25E-07**	1.8E-07	**1.93E-14**	1.0E-05	**1.12E-08**	7.9E-06	**4.87E-08**	8.0E-08	**3.04E-14**	5.0E-06	**9.11E-09**	7.9E-06	**2.93E-08**
1.65	1.1E-08	**7.89E-18**	4.5E-06	**5.71E-08**	6.7E-06	**1.89E-07**	5.8E-08	**2.55E-15**	9.4E-06	**1.39E-08**	7.8E-06	**6.43E-08**	2.2E-08	**3.88E-13**	7.3E-06	**1.10E-08**	9.6E-06	**3.50E-08**
1.7	3.1E-09	**3.12E-15**	4.2E-06	**5.89E-08**	5.7E-06	**1.54E-07**	3.7E-10	**2.53E-16**	4.9E-06	**1.31E-08**	7.0E-06	**4.79E-08**	5.7E-07	**7.16E-16**	7.0E-06	**8.33E-09**	9.6E-06	**2.37E-08**
1.75	1.9E-08	**2.39E-12**	3.0E-06	**4.17E-08**	3.5E-06	**6.21E-08**	2.0E-07	**2.16E-13**	7.0E-06	**8.05E-09**	6.2E-06	**1.68E-08**	6.6E-08	**2.28E-13**	4.1E-06	**3.08E-09**	7.0E-06	**6.42E-09**
1.8	7.2E-10	**3.11E-12**	1.5E-06	**1.80E-08**	1.4E-06	**2.76E-08**	1.8E-06	**9.36E-15**	1.6E-05	**3.38E-09**	5.9E-06	**5.67E-09**	3.8E-07	**1.03E-14**	8.2E-06	**1.33E-09**	4.4E-06	**2.54E-09**
1.85	2.3E-09	**5.70E-14**	2.9E-06	**3.18E-08**	4.0E-06	**1.04E-07**	3.8E-06	**5.45E-14**	1.9E-05	**8.39E-09**	4.9E-06	**3.76E-08**	2.5E-06	**1.93E-12**	1.6E-05	**8.50E-09**	6.7E-06	**2.76E-08**
1.9	3.8E-08	**4.71E-12**	5.5E-06	**1.03E-07**	7.3E-06	**2.60E-07**	4.6E-08	**5.25E-14**	7.1E-06	**2.41E-08**	6.7E-06	**8.64E-08**	1.6E-07	**3.53E-14**	1.2E-05	**1.96E-08**	1.2E-05	5.96E-08
1.95	4.7E-08	**1.32E-12**	7.2E-06	**1.08E-07**	8.9E-06	**1.83E-07**	6.5E-07	**1.18E-13**	2.2E-05	**2.29E-08**	1.2E-05	**5.78E-08**	8.8E-07	**3.02E-12**	1.8E-05	**1.41E-08**	1.1E-05	**3.80E-08**
2	1.0E-08	**1.32E-13**	6.1E-06	**1.71E-08**	7.2E-06	**5.12E-08**	4.8E-06	**8.53E-15**	3.9E-05	**4.29E-09**	1.3E-05	**1.70E-08**	9.2E-07	**2.76E-15**	3.8E-05	**4.23E-09**	1.1E-05	**1.31E-08**

Table 13. Statistical analysis of the results obtained by the LNN-GNDO-SQP algorithm, GA-ASA technique on the 21 steps within the interval [1 2], It is evident that LNN-GNDO-SQP is superior in accuracy and stability. Three cases of drainage problem are considered based on variations in a.

	Case I						Case II						Case III					
	Min		Mean		Std		Min		Mean		Std		Min		Mean		Std	
	GA-ASA	GNDO-SQP	GA-ASA	GNDO-SQP	GA-ASA	GNDO-SQP	GA-ASA	GNDO-SQP	GA-ASA	GNDO-SQP	GA-ASA	GNDO-SQP	GA-ASA	GNDO-SQP	GA-ASA	GNDO-SQP	GA-ASA	GNDO-SQP
1	**4.0E-12**	6.40E-12	4.3E-07	**2.20E-07**	9.5E-07	**5.57E-07**	6.8E-12	**9.89E-15**	1.1E-07	1.28E-06	**3.5E-07**	3.42E-06	**5.2E-11**	8.73E-11	**2.4E-07**	8.80E-07	**6.5E-07**	2.37E-06
1.05	2.5E-08	**8.59E-10**	2.0E-06	**4.40E-07**	2.3E-06	**5.55E-07**	3.3E-08	**3.67E-11**	4.4E-06	**3.48E-06**	**2.0E-06**	5.00E-06	4.1E-07	**3.05E-12**	1.8E-05	**3.95E-06**	**5.2E-06**	6.93E-06
1.1	1.3E-08	**1.22E-10**	5.1E-06	**6.69E-07**	6.4E-06	**1.28E-06**	2.6E-07	**5.24E-12**	9.4E-06	**4.85E-06**	**4.3E-06**	1.01E-05	4.9E-07	**1.43E-09**	3.3E-05	**3.86E-06**	1.0E-05	**9.21E-06**
1.15	1.2E-08	**1.90E-13**	6.6E-06	**3.18E-07**	9.5E-06	**8.56E-07**	4.0E-08	**1.70E-11**	9.5E-06	**2.16E-06**	**4.6E-06**	6.28E-06	4.8E-07	**1.31E-10**	2.9E-05	**1.55E-06**	9.6E-06	**4.05E-06**
1..20	2.7E-08	**2.32E-10**	6.2E-06	**7.41E-08**	1.0E-05	**1.89E-07**	1.3E-07	**1.91E-11**	6.3E-06	**4.91E-07**	3.5E-06	**1.22E-06**	9.7E-07	**3.05E-12**	1.6E-05	**2.93E-07**	5.4E-06	**4.64E-07**
1.25	7.3E-09	**6.34E-11**	4.7E-06	**9.85E-08**	9.2E-06	**1.09E-07**	4.7E-08	**2.36E-13**	2.8E-06	**8.42E-07**	2.2E-06	**9.36E-07**	1.4E-06	**9.13E-11**	6.6E-06	**2.81E-07**	1.4E-06	**4.16E-07**
1.3	3.1E-08	**3.52E-13**	3.0E-06	**2.11E-07**	6.8E-06	**3.00E-07**	1.7E-08	**6.64E-12**	**1.1E-06**	1.75E-06	**1.2E-06**	2.52E-06	9.5E-07	**1.61E-11**	7.7E-06	**9.46E-07**	**1.9E-06**	2.19E-06
1.35	2.1E-08	**4.19E-12**	1.9E-06	**2.51E-07**	4.2E-06	**5.70E-07**	8.3E-08	**6.87E-12**	**1.7E-06**	2.00E-06	**9.4E-07**	4.68E-06	3.6E-08	**8.31E-12**	1.7E-05	**1.59E-06**	**2.6E-06**	4.01E-06
1.4	2.4E-08	**3.65E-14**	1.8E-06	**2.01E-07**	2.4E-06	**5.81E-07**	2.6E-07	**4.51E-13**	4.3E-06	**1.54E-06**	**1.8E-06**	4.80E-06	7.5E-07	**1.41E-11**	2.8E-05	**1.70E-06**	5.6E-06	**4.35E-06**
1.45	1.4E-08	**5.93E-11**	2.2E-06	**1.23E-07**	2.0E-06	**3.23E-07**	1.4E-07	**4.92E-14**	7.5E-06	**9.47E-07**	3.2E-06	**2.73E-06**	5.8E-07	**1.52E-12**	3.5E-05	**1.18E-06**	1.0E-05	**2.94E-06**
1.5	3.1E-08	**2.86E-14**	2.7E-06	**7.57E-08**	2.2E-06	**9.79E-08**	9.9E-08	**2.21E-12**	9.9E-06	**6.79E-07**	4.3E-06	**8.02E-07**	6.0E-07	**1.79E-11**	3.6E-05	**4.36E-07**	1.3E-05	**9.16E-07**
1.55	9.5E-09	**1.90E-13**	3.5E-06	**7.83E-08**	3.0E-06	**1.00E-07**	2.1E-07	**4.34E-13**	1.1E-05	**7.58E-07**	4.8E-06	**9.57E-07**	1.6E-06	**1.42E-12**	3.2E-05	**1.06E-07**	1.4E-05	**1.94E-07**
1.6	6.3E-09	**2.29E-11**	4.5E-06	**1.18E-07**	4.8E-06	**2.26E-07**	2.9E-07	**6.22E-14**	9.6E-06	**9.97E-07**	4.6E-06	**1.81E-06**	3.2E-07	**4.07E-12**	2.4E-05	**5.56E-07**	1.3E-05	**1.24E-06**
1.65	1.6E-08	**3.14E-13**	5.3E-06	**1.65E-07**	7.1E-06	**4.56E-07**	4.3E-07	**1.65E-13**	7.3E-06	**1.25E-06**	3.9E-06	**3.75E-06**	1.5E-06	**4.07E-13**	1.8E-05	**1.43E-06**	9.1E-06	**3.51E-06**
1.7	1.6E-08	**3.26E-13**	5.7E-06	**1.79E-07**	9.1E-06	**4.55E-07**	1.5E-08	**2.41E-16**	4.6E-06	**1.39E-06**	3.4E-06	**3.83E-06**	9.9E-07	**2.62E-12**	1.4E-05	**1.83E-06**	4.7E-06	**4.42E-06**
1.75	1.8E-08	**2.33E-12**	5.7E-06	**1.31E-07**	9.9E-06	**2.17E-07**	1.0E-07	**5.04E-15**	2.7E-06	**1.18E-06**	3.3E-06	**1.87E-06**	3.7E-07	**2.47E-13**	1.5E-05	**1.18E-06**	2.9E-06	**2.64E-06**
1.8	2.8E-08	**1.47E-10**	5.2E-06	**5.55E-08**	9.2E-06	**8.26E-08**	4.2E-08	**6.13E-13**	2.1E-06	**6.15E-07**	2.9E-06	**8.15E-07**	1.3E-06	**3.18E-11**	1.8E-05	**1.81E-07**	3.8E-06	**2.78E-07**
1.85	1.8E-08	**3.05E-13**	4.1E-06	**8.36E-08**	7.1E-06	**2.16E-07**	1.6E-08	**3.94E-14**	2.7E-06	**6.04E-07**	2.0E-06	**1.63E-06**	1.2E-06	**2.68E-12**	2.2E-05	**5.76E-07**	3.9E-06	**1.38E-06**
1.9	2.8E-08	**2.29E-11**	2.9E-06	**2.94E-07**	4.4E-06	**6.77E-07**	3.8E-09	**7.23E-13**	5.3E-06	**2.26E-06**	**2.4E-06**	5.31E-06	2.5E-08	**2.23E-13**	2.5E-05	**2.70E-06**	**6.1E-06**	6.31E-06
1.95	1.4E-08	**4.23E-10**	2.8E-06	**3.31E-07**	2.7E-06	**5.35E-07**	2.1E-07	**3.51E-11**	8.8E-06	**2.99E-06**	3.9E-06	**1.30E-06**	1.8E-06	**3.90E-10**	2.5E-05	**2.70E-06**	1.1E-05	**5.81E-06**
2	4.9E-08	**6.30E-13**	3.0E-06	**4.73E-08**	2.6E-06	**1.20E-07**	1.4E-07	**3.27E-14**	9.7E-06	**3.57E-07**	4.4E-06	**9.54E-07**	2.3E-08	**3.11E-14**	2.4E-05	**3.96E-07**	1.3E-05	**9.24E-07**

Table 14. Fitness values, MAD,TIC RMSE and ENSE for SCENARIO I of drainage problem

	Fit			MAD			TIC			RMSE			ENSE		
Cases	Min.	Mean	Std.	Min.	Mean	Std.	Min.	Mean	Std.	Min.	Mean	Std.	Min.	Mean	Std.
I	1.49E-12	1.63E-09	4.68E-09	4.99E-08	1.84E-06	2.44E-06	2.49E-07	9.04E-06	1.23E-05	6.13E-08	2.22E-06	3.03E-06	1.36E-10	5.07E-07	1.46E-06
II	1.20E-11	3.96E-08	8.33E-08	1.70E-07	8.94E-06	1.05E-05	2.51E-07	1.47E-05	1.76E-05	1.85E-07	1.09E-05	1.30E-05	1.76E-10	1.15E-06	2.59E-06
III	4.51E-12	6.43E-08	1.30E-07	2.12E-07	1.08E-05	1.12E-05	2.59E-07	1.35E-05	1.42E-05	2.55E-07	1.33E-05	1.40E-05	1.54E-10	8.26E-07	1.72E-06

Table 15. Fitness values, MAD,TIC RMSE and ENSE for SCENARIO II of drainage problem

	Fit			MAD			TIC			RMSE			ENSE		
Cases	Min.	Mean	Std.	Min.	Mean	Std.	Min.	Mean	Std.	Min.	Mean	Std.	Min.	Mean	Std.
I	4.34E-11	1.18E-07	2.35E-07	1.86E-07	1.87E-05	1.98E-05	1.86E-07	1.81E-05	1.96E-05	2.29E-07	2.22E-05	2.41E-05	7.57E-11	1.61E-06	3.32E-06
II	1.05E-10	2.78E-07	6.38E-07	2.67E-07	2.28E-05	2.58E-05	2.59E-07	2.18E-05	2.53E-05	3.31E-07	2.79E-05	3.24E-05	1.47E-10	2.43E-06	5.93E-06
III	1.50E-09	3.21E-07	6.88E-07	3.51E-07	1.66E-05	1.76E-05	3.10E-07	1.49E-05	1.55E-05	4.23E-07	2.03E-05	2.11E-05	2.29E-10	1.08E-06	2.60E-06

Table 16. Fitness values, MAD,TIC RMSE and ENSE for SCENARIO III of drainage problem

	Fit			MAD			TIC			RMSE			ENSE		
Cases	Min.	Mean	Std.	Min.	Mean	Std.	Min.	Mean	Std.	Min.	Mean	Std.	Min.	Mean	Std.
I	6.63E-12	6.37E-08	1.48E-07	3.67E-07	1.45E-05	1.53E-05	3.54E-07	1.46E-05	1.57E-05	4.35E-07	1.79E-05	1.93E-05	2.95E-10	9.69E-07	2.16E-06
II	1.08E-12	1.42E-08	4.90E-08	1.76E-07	4.45E-06	6.15E-06	1.93E-07	5.09E-06	7.07E-06	2.10E-07	5.53E-06	7.68E-06	8.21E-11	1.52E-07	5.00E-07
III	1.08E-12	9.66E-09	2.72E-08	2.82E-07	3.52E-06	5.31E-06	3.51E-07	4.30E-06	6.37E-06	3.53E-07	4.32E-06	6.40E-06	2.39E-10	1.21E-07	3.61E-07

Table 17. Fitness values, MAD,TIC RMSE and ENSE for SCENARIO IV of drainage problem

	Fit			MAD			TIC			RMSE			ENSE		
Cases	Min.	Mean	Std.	Min.	Mean	Std.	Min.	Mean	Std.	Min.	Mean	Std.	Min.	Mean	Std.
I	7.66E-11	1.95E-07	3.96E-07	2.25E-06	3.62E-05	3.49E-05	1.43E-06	2.49E-05	2.45E-05	2.47E-06	4.29E-05	4.23E-05	5.63E-09	2.81E-06	5.56E-06
II	3.20E-12	1.47E-06	3.08E-06	3.17E-06	8.21E-05	8.21E-05	1.99E-06	5.13E-05	5.26E-05	3.90E-06	0.000101	0.000103	9.23E-09	1.23E-05	2.57E-05
III	5.00E-09	1.25E-06	2.93E-06	4.37E-06	4.59E-05	6.62E-05	2.31E-06	2.48E-05	3.57E-05	4.99E-06	5.36E-05	7.72E-05	1.50E-08	5.05E-06	1.17E-05

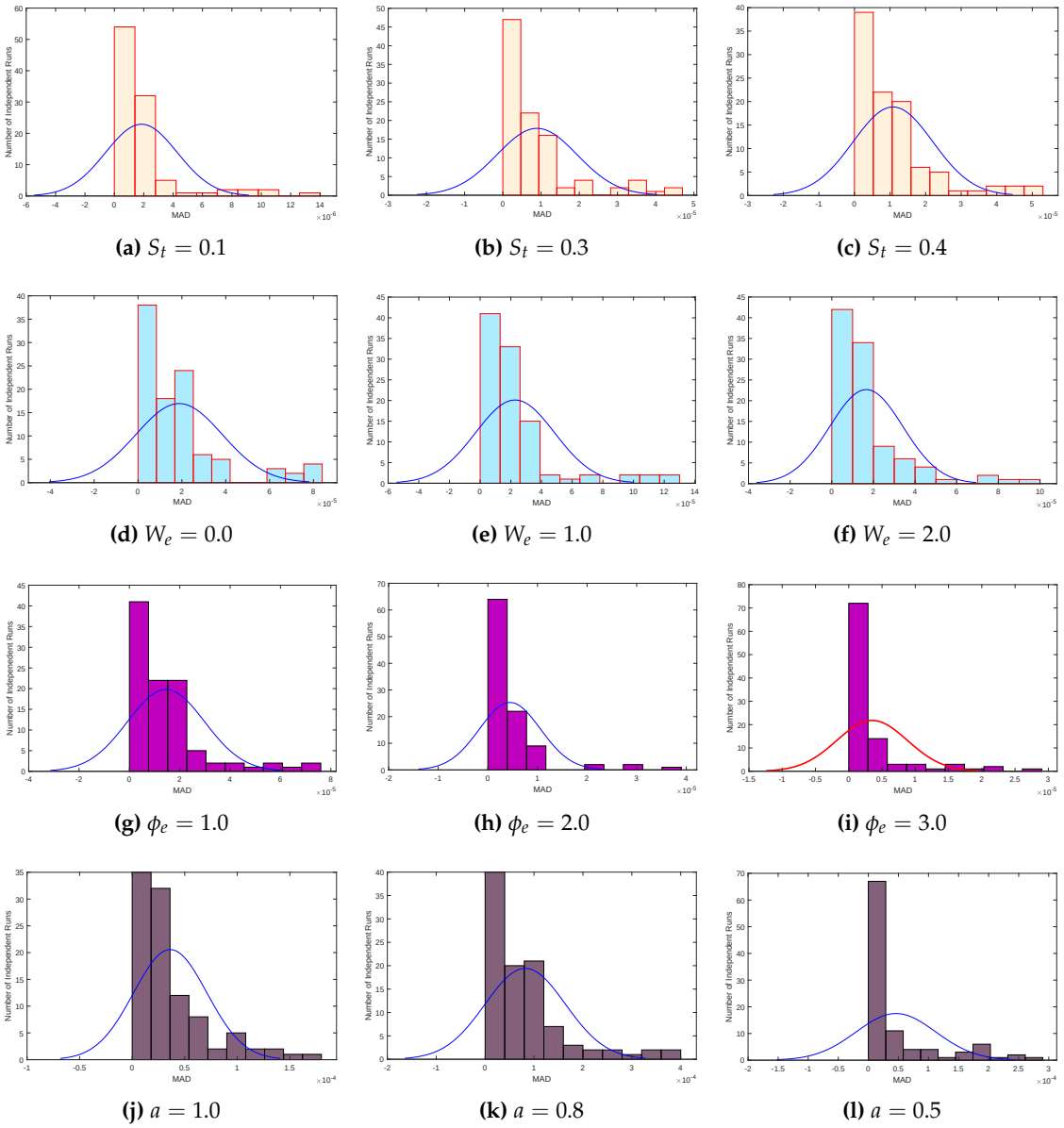

(a) $S_t = 0.1$ **(b)** $S_t = 0.3$ **(c)** $S_t = 0.4$

(d) $W_e = 0.0$ **(e)** $W_e = 1.0$ **(f)** $W_e = 2.0$

(g) $\phi_e = 1.0$ **(h)** $\phi_e = 2.0$ **(i)** $\phi_e = 3.0$

(j) $a = 1.0$ **(k)** $a = 0.8$ **(l)** $a = 0.5$

Figure 10. Histograms of MAD values with normal distribution fit for four scenarios of drainage problem.

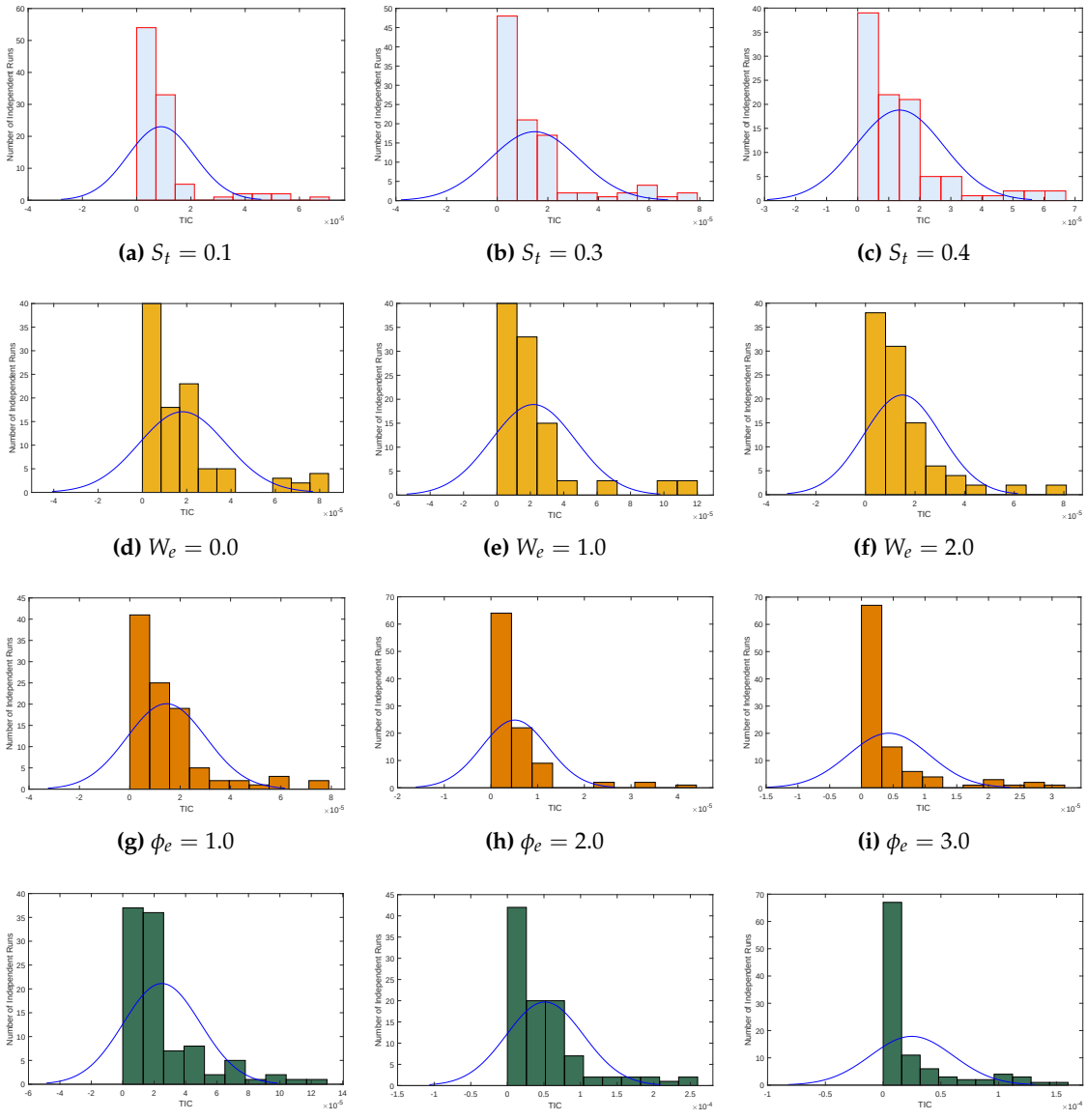

(a) $S_t = 0.1$ **(b)** $S_t = 0.3$ **(c)** $S_t = 0.4$

(d) $W_e = 0.0$ **(e)** $W_e = 1.0$ **(f)** $W_e = 2.0$

(g) $\phi_e = 1.0$ **(h)** $\phi_e = 2.0$ **(i)** $\phi_e = 3.0$

(j) $a = 1.0$ **(k)** $a = 0.8$ **(l)** $a = 0.5$

Figure 11. Histograms of TIC values with normal distribution fit for four scenarios of drainage problem.

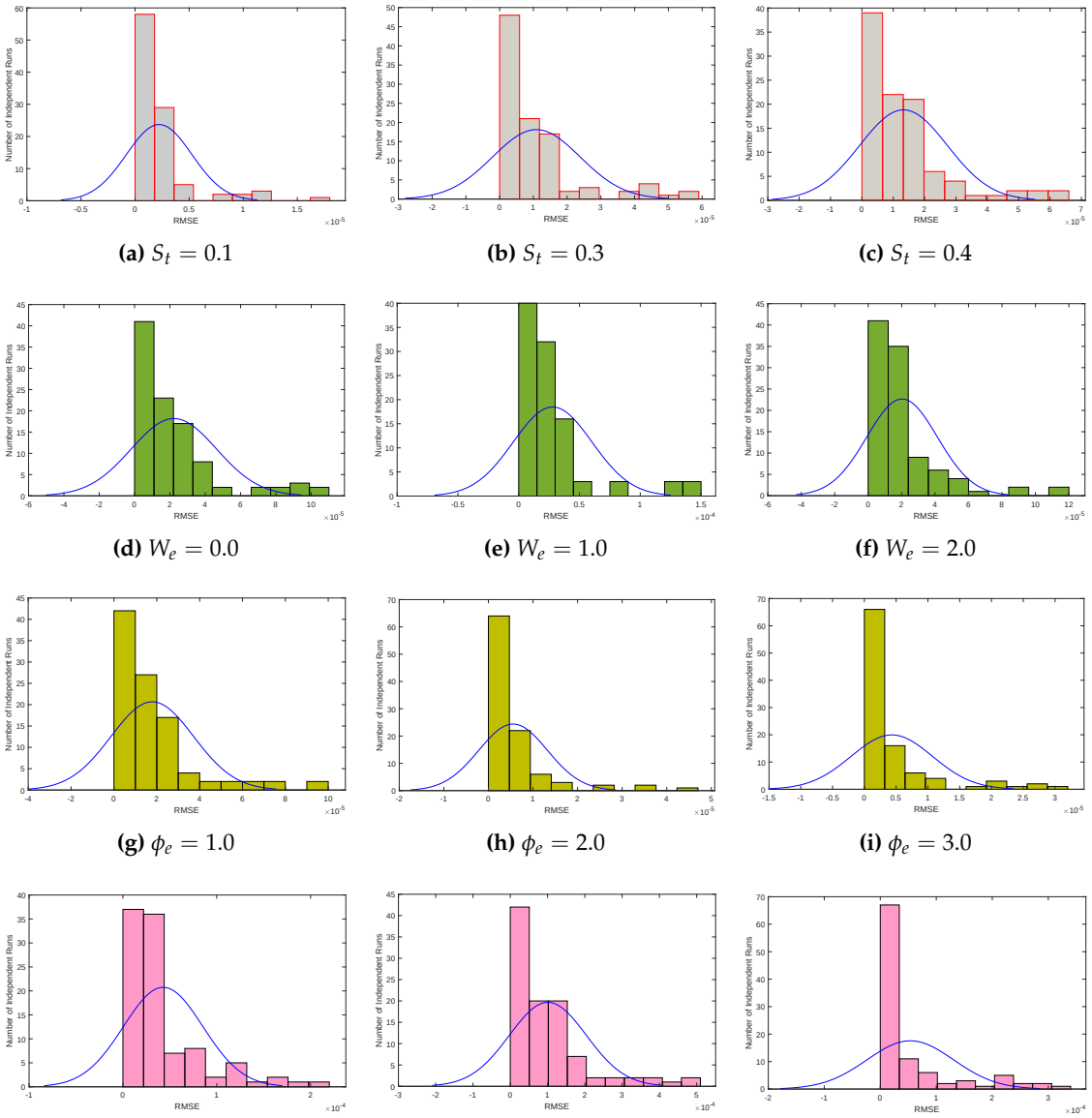

(a) $S_t = 0.1$ **(b)** $S_t = 0.3$ **(c)** $S_t = 0.4$

(d) $W_e = 0.0$ **(e)** $W_e = 1.0$ **(f)** $W_e = 2.0$

(g) $\phi_e = 1.0$ **(h)** $\phi_e = 2.0$ **(i)** $\phi_e = 3.0$

(j) $a = 1.0$ **(k)** $a = 0.8$ **(l)** $a = 0.5$

Figure 12. Histograms of RMSE values with normal distribution fit for four scenarios of drainage problem.

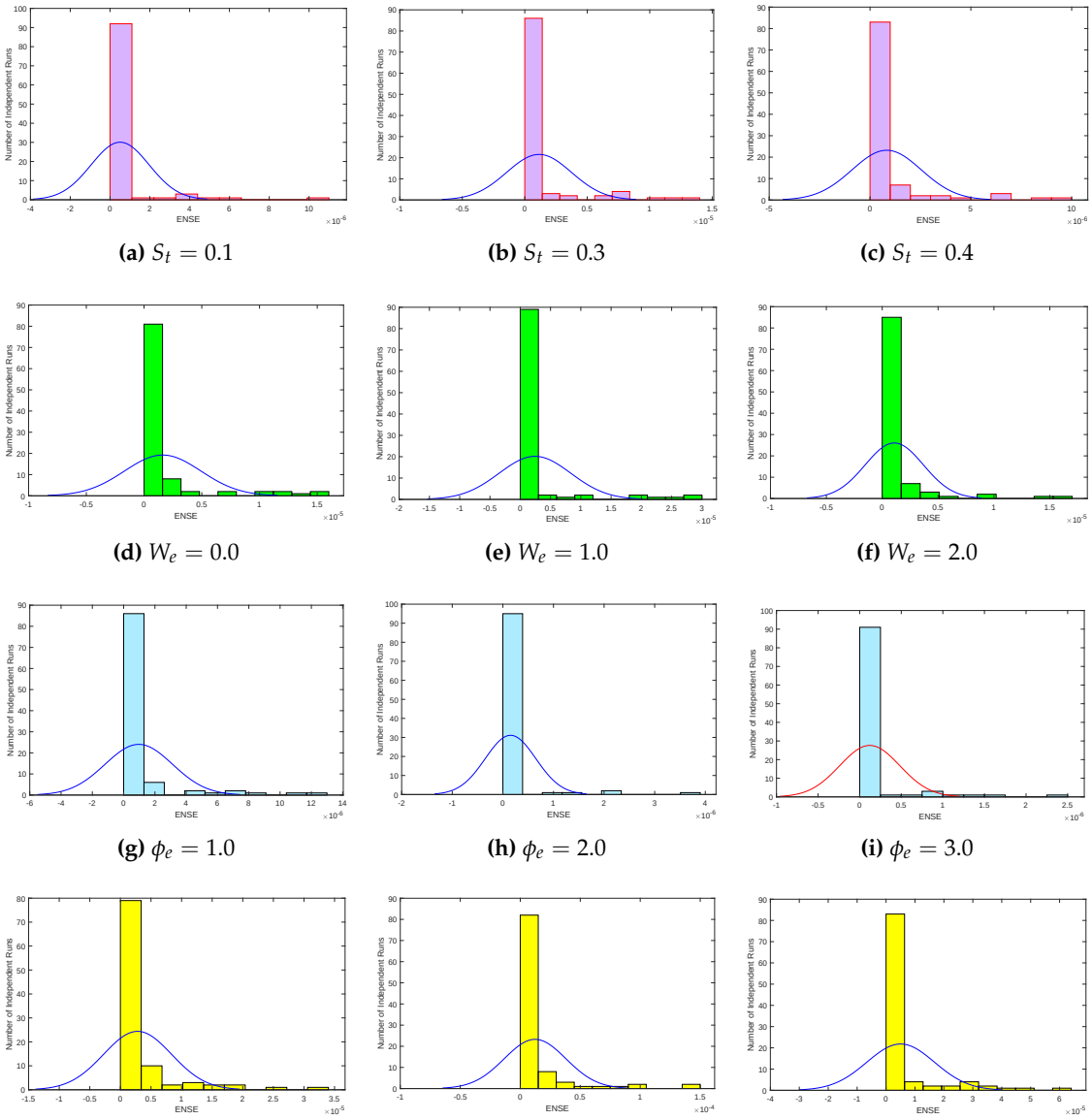

(a) $S_t = 0.1$ **(b)** $S_t = 0.3$ **(c)** $S_t = 0.4$

(d) $W_e = 0.0$ **(e)** $W_e = 1.0$ **(f)** $W_e = 2.0$

(g) $\phi_e = 1.0$ **(h)** $\phi_e = 2.0$ **(i)** $\phi_e = 3.0$

(j) $a = 1.0$ **(k)** $a = 0.8$ **(l)** $a = 0.5$

Figure 13. Histograms of ENSE values with normal distribution fit for four scenarios of drainage problem.

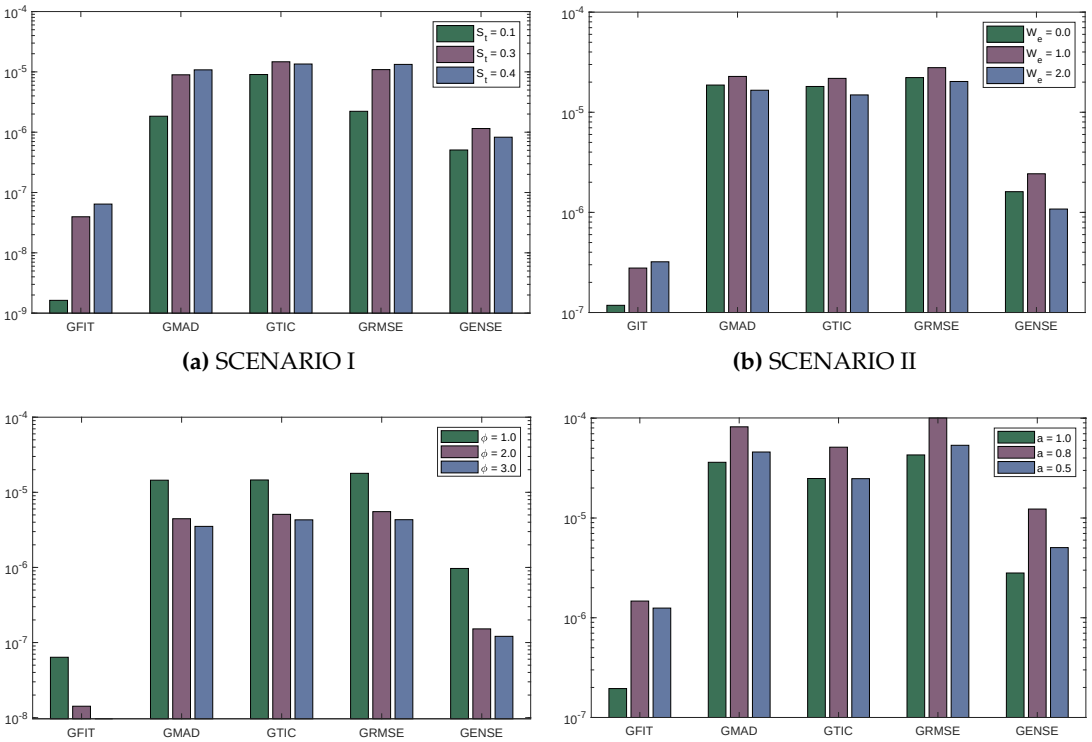

(a) SCENARIO I **(b)** SCENARIO II

(c) SCENARIO III **(d)** SCENARIO IV

Figure 14. Global performance indicators for four scenarios of drainage problem.

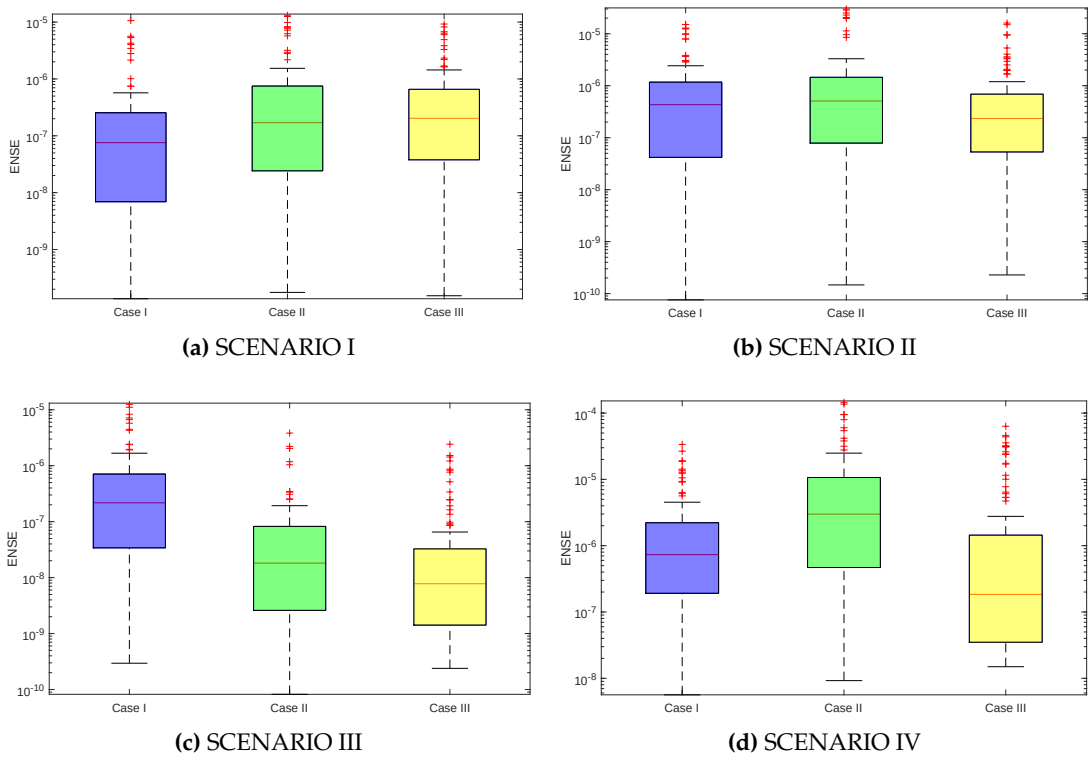

(a) SCENARIO I **(b)** SCENARIO II

(c) SCENARIO III **(d)** SCENARIO IV

Figure 15. Boxplots showing distribution of ENSE values for four scenarios of drainage problem.

7. Conclusion

This paper has investigated steady thin film flow of magnetohydrodynamic (MHD) non-Newtonian fluid on the vertical cylinder's outer surface used in drainage problems. The drainage problem is mathematically modeled using basic concepts of continuity and momentum equation that results in partial differential equations. Furthermore, the problem is reduced to a nonlinear ordinary differential equation by incorporating a similarity transformation technique. To study the velocity profile of Johnson Segalman fluid under the influence of variations in Stokes number, Weissenberg numbers, ratio of viscosities, and slip parameter, a novel heuristic soft computing technique is developed. The proposed technique is named as LNN-GNDO-SQP algorithm that combines unsupervised learning of GNDO and supervised strategy of SQP.

We conclude our findings and mathematical analysis as follows.

• A novel soft computing technique is designed in which Legendre polynomials are weighted with neurons in artificial neural networks (ANN) that is used to model approximate solutions for Eq (29). In Eq (29), in order to determine the accuracy of candidate solutions, fitness functions are constructed. We have used an efficient global search mechanism, namely, generalized normal distribution optimization (GNDO), and a local search technique known as sequential quadratic programming algorithm to minimize the fitness function. Our proposed algorithm is named the LNN-GNDO-SQP algorithm.

• Better approximate series solutions are calculated for different cases of each scenario shown in Figure 5. Our results are validated by comparing the statistical values of absolute errors in term of minimum, mean, and standard deviation obtained by the proposed algorithm with the GA-ASA algorithm as shown in Tables 10-13.

• We have investigated the variations in velocity profile due to Stokes number and Weissenberg numbers changes. It is established that changes in velocity profile are directly proportional to Stokes number and Weissenberg numbers. In contrast, variations in the ratio of viscosities and slip parameter have an inverse relation with the velocity profile.

• Extensive statistical and graphical analysis for drainage problems illustrates the stability, efficiency, and effectiveness of the proposed algorithm in solving real-world problems. In the future, the LNN-GNDO-SQP algorithm can be used to solve problems involving systems of differential equations.

8. Acknowledgment

This project was funded by the Deanship of Scientific Research, King Abdulaziz University, Jeddah, under grant No. (DF-232-135-1441). The author, therefore, gratefully acknowledge DSR technical and financial supports.

9. Appendix

Approximate series solutions obtained by LNN-GNDO-SQP algorithm for different cases of scenario I.

Case I

$$w(r) = -0.267240 + (0.083281r + 0.361633)(0.199856) + \ldots + \left(\frac{90090(-0.225430r + 0.133951)^6 - 30030(-0.225430r + 0.133951)^4 + 3465(-0.225430r + 0.133951)^2 - 63}{256}\right)(-0.362530) \tag{A1}$$

Case II

$$u_{approx}(\xi) = -0.161130 + (-0.082950r - 0.133580)(0.540048) + \ldots + \left(\frac{90090(0.041990r + 0.288770)^6 - 30030(0.041990r + 0.288770)^4 + 3465(0.041990r + 0.288770)^2 - 63}{256}\right)(0.999719) \tag{A2}$$

Case III

$$u_{approx}(\xi) = -0.642690 + (-0.085350r + 0.282074)(-0.500960) + \ldots + \left(\frac{90090(-0.229960r - 0.050250)^6 - 30030(-0.229960r - 0.050250)^4 + 3465(-0.229960r - 0.050250)^2 - 63}{256}\right)(-0.148830) \tag{A3}$$

Approximate series solutions obtained by LNN-GNDO-SQP algorithm for different cases of scenario II.

Case I

$$w(r) = -0.277180 + (0.9900770r - 0.999960)(-0.744240) + \dots + \left(\frac{90090(-0.744240r + 0.101130)^6 - 30030(-0.744240r + 0.101130)^4 + 3465(-0.744240r + 0.101130)^2 - 63}{256}\right)(-0.629380) \tag{A4}$$

Case II

$$u_{approx}(\xi) = -0.984680 + (0.555550r - 0.024790)(-0.801200) + \dots + \left(\frac{90090(-0.138270r + 0.103016)^6 - 30030(-0.138270r + 0.103016)^4 + 3465(-0.138270r + 0.103016)^2 - 63}{256}\right)(-0.138360) \tag{A5}$$

Case III

$$u_{approx}(\xi) = -0.575380 + (0.131423r + 0.343622)(-0.999990) + \dots + \left(\frac{90090(0.174965r + 0.126845)^6 - 30030(0.174965r + 0.126845)^4 + 3465(0.174965r + 0.126845)^2 - 63}{256}\right)(-0.148830) \tag{A6}$$

Approximate series solutions obtained by LNN-GNDO-SQP algorithm for different cases of scenario III.

Case I

$$u_{approx}(\xi) = -0.578170 + (-0.552250r + 0.999977)(0.64279) + \dots + \left(\frac{90090(0.270983r - 0.10505)^6 - 30030(0.270983r - 0.10505)^4 + 3465(0.270983r - 0.10505)^2 - 63}{256}\right)(-0.148830) \tag{A7}$$

Case II

$$u_{approx}(\xi) = -0.719570 + (-0.300220r + 0.348017)(0.863347) + \dots + \left(\frac{90090(0.188646r - 0.08349)^6 - 30030(0.188646r - 0.08349)^4 + 3465(0.188646r - 0.08349)^2 - 63}{256}\right)(0.161173) \tag{A8}$$

Case III

$$u_{approx}(\xi) = -0.84187 + (0.271674r + 0.687734)(0.456016) + \dots + \left(\frac{90090(0.271897r + 0.005882)^6 - 30030(0.271897r + 0.005882)^4 + 3465(0.271897r + 0.005882)^2 - 63}{256}\right)(-0.547840) \tag{A9}$$

Approximate series solutions obtained by LNN-GNDO-SQP algorithm for different cases of scenario IV.

Case I

$$u_{approx}(\xi) = -0.937800 + (-0.384460r - 0.286000)(0.373960) + \dots + \left(\frac{90090(-0.212490r + 0.046098)^6 - 30030(-0.212490r + 0.046098)^4 + 3465(-0.212490r + 0.046098)^2 - 63}{256}\right)(-0.080280) \tag{A10}$$

Case II

$$u_{approx}(\xi) = -0.996410 + (0.389527r + 0.441955)(0.308871) + \dots + \left(\frac{90090(0.295517r - 1.000000)^6 - 30030(0.295517r - 1.000000)^4 + 3465(0.295517r - 1.000000)^2 - 63}{256}\right)(-0.616560) \tag{A11}$$

Case III

$$u_{approx}(\xi) = -1.357140 + (-0.810600r - 0.543930)(1.620159) + \dots + \left(\frac{90090(-0.266330r - 0.063730)^6 - 30030(-0.266330r - 0.063730)^4 + 3465(-0.266330r - 0.063730)^2 - 63}{256}\right)(-1.171850) \tag{A12}$$

References

1. Munson, B.; Young, D.; Okiishi, T.; Huebsch, W. Finite control volume analysis. *Fundamentals of fluid mechanics, second ed. Wiley, NewYork* **1994**, pp. 211–306.
2. Landau, L. EM Lifshitz, Fluid Mechanics. *Course of theoretical physics* **1959**, *6*.
3. Siddiqui, A.M.; Mahmood, R.; Ghori, Q. Homotopy perturbation method for thin film flow of a fourth grade fluid down a vertical cylinder. *Physics Letters A* **2006**, *352*, 404–410.
4. Siddiqui, A.M.; Mahmood, R.; Ghori, Q. Some exact solutions for the thin film flow of a PTT fluid. *Physics Letters A* **2006**, *356*, 353–356.
5. Alam, M.K.; Rahim, M.T.; Haroon, T.; Islam, S.; Siddiqui, A.M. Solution of steady thin film flow of Johnson–Segalman fluid on a vertical moving belt for lifting and drainage problems using Adomian Decomposition Method. *Applied Mathematics and Computation* **2012**, *218*, 10413–10428.

6. Alam, M.K.; Rahim, M.T.; Avital, E.; Islam, S.; Siddiqui, A.M.; Williams, J. Solution of the steady thin film flow of non-Newtonian fluid on vertical cylinder using Adomian Decomposition Method. *Journal of the Franklin Institute* **2013**, *350*, 818–839.
7. Johnson Jr, M.; Segalman, D. A model for viscoelastic fluid behavior which allows non-affine deformation. *Journal of Non-Newtonian fluid mechanics* **1977**, *2*, 255–270.
8. McLeish, T.; Ball, R. A molecular approach to the spurt effect in polymer melt flow. *Journal of Polymer Science Part B: Polymer Physics* **1986**, *24*, 1735–1745.
9. Kolkka, R.; Malkus, D.; Hansen, M.; Ierley, G. Spurt phenomena of the Johnson-Segalman fluid and related models. *Journal of Non-Newtonian Fluid Mechanics* **1988**, *29*, 303–335.
10. Malkus, D.S.; Nohel, J.A.; Plohr, B.J. Dynamics of shear flow of a non-Newtonian fluid. *Journal of Computational Physics* **1990**, *87*, 464–487.
11. Rao, I. Flow of a Johnson–Segalman fluid between rotating co-axial cylinders with and without suction. *International journal of non-linear mechanics* **1999**, *34*, 63–70.
12. Rao, I.; Rajagopal, K. Some simple flows of a Johnson-Segalman fluid. *Acta mechanica* **1999**, *132*, 209–219.
13. Hayat, T.; Wang, Y.; Siddiqui, A.M.; Hutter, K. Peristaltic motion of a Johnson-Segalman fluid in a planar channel. *Mathematical Problems in Engineering* **2003**, *2003*.
14. Bougoffa, L.; Rach, R.; Wazwaz, A.M.; Duan, J.S. On the Adomian decomposition method for solving the Stefan problem. *International Journal of Numerical Methods for Heat & Fluid Flow* **2015**.
15. Fatoorehchi, H.; Abolghasemi, H. Approximating the minimum reflux ratio of multicomponent distillation columns based on the Adomian decomposition method. *Journal of the Taiwan Institute of Chemical Engineers* **2014**, *45*, 880–886.
16. Wazwaz, A.M. The variational iteration method for solving linear and nonlinear ODEs and scientific models with variable coefficients. *Central European Journal of Engineering* **2014**, *4*, 64–71.
17. Kouhi, M.; Oñate, E. A stabilized finite element formulation for high-speed inviscid compressible flows using finite calculus. *International Journal for Numerical Methods in Fluids* **2014**, *74*, 872–897.
18. Marsden, O.; Bogey, C.; Bailly, C. A study of infrasound propagation based on high-order finite difference solutions of the Navier-Stokes equations. *The Journal of the Acoustical Society of America* **2014**, *135*, 1083–1095.
19. Marinca, V.; Herişanu, N. Nonlinear dynamic analysis of an electrical machine rotor–bearing system by the optimal homotopy perturbation method. *Computers & Mathematics with Applications* **2011**, *61*, 2019–2024.
20. Herişanu, N.; Marinca, V. Optimal homotopy perturbation method for a non-conservative dynamical system of a rotating electrical machine. *Zeitschrift für Naturforschung A* **2012**, *67*, 509–516.
21. Sobamowo, G.M. On Heat transfer analysis in pipe flow of Johnson-Segalman Fluid: Analytical Solution and Parametric Studies. *AUT Journal of Mechanical Engineering* **2019**, *3*, 187–196.
22. Hayat, T.; Aslam, N.; Khan, M.I.; Khan, M.I.; Alsaedi, A. MHD peristaltic motion of Johnson–Segalman fluid in an inclined channel subject to radiative flux and convective boundary conditions. *Computer methods and programs in biomedicine* **2019**, *180*, 104999.
23. Bukhari, A.H.; Sulaiman, M.; Raja, M.A.Z.; Islam, S.; Shoaib, M.; Kumam, P. Design of a hybrid NAR-RBFs neural network for nonlinear dusty plasma system. *Alexandria Engineering Journal* **2020**, *59*, 3325–3345.
24. Ahmad, A.; Sulaiman, M.; Alhindi, A.; Aljohani, A.J. Analysis of temperature profiles in longitudinal fin designs by a novel neuroevolutionary approach. *IEEE Access* **2020**, *8*, 113285–113308.
25. Khan, N.A.; Sulaiman, M.; Aljohani, A.J.; Kumam, P.; Alrabaiah, H. Analysis of Multi-Phase Flow Through Porous Media for Imbibition Phenomena by Using the LeNN-WOA-NM Algorithm. *IEEE Access* **2020**, *8*, 196425–196458.
26. Ali, A.; Qadri, S.; Khan Mashwani, W.; Kumam, W.; Kumam, P.; Naeem, S.; Goktas, A.; Jamal, F.; Chesneau, C.; Anam, S.; others. Machine Learning Based Automated Segmentation and Hybrid Feature Analysis for Diabetic Retinopathy Classification Using Fundus Image. *Entropy* **2020**, *22*, 567.
27. Waseem, W.; Sulaiman, M.; Alhindi, A.; Alhakami, H. A Soft Computing Approach Based on Fractional Order DPSO Algorithm Designed to Solve the Corneal Model for Eye Surgery. *IEEE Access* **2020**, *8*, 61576–61592.
28. Zhang, Y.; Jin, Z.; Mirjalili, S. Generalized normal distribution optimization and its applications in parameter extraction of photovoltaic models. *Energy Conversion and Management* **2020**, *224*, 113301.
29. Nocedal, J.; Wright, S. *Numerical optimization*; Springer Science & Business Media, 2006.

30. Garcea, G.; Bilotta, A.; Leonetti, L. An efficient algorithm for shakedown analysis based on equality constrained sequential quadratic programming. In *Direct Methods for Limit and Shakedown Analysis of Structures*; Springer, 2015; pp. 177–197.
31. Morshed, M.J.; Asgharpour, A. Hybrid imperialist competitive-sequential quadratic programming (HIC-SQP) algorithm for solving economic load dispatch with incorporating stochastic wind power: a comparative study on heuristic optimization techniques. *Energy conversion and management* **2014**, *84*, 30–40.
32. Badreddine, H.; Vandewalle, S.; Meyers, J. Sequential quadratic programming (SQP) for optimal control in direct numerical simulation of turbulent flow. *Journal of Computational Physics* **2014**, *256*, 1–16.
33. Raja, M.A.Z.; Shah, F.H.; Khan, A.A.; Khan, N.A. Design of bio-inspired computational intelligence technique for solving steady thin film flow of Johnson–Segalman fluid on vertical cylinder for drainage problems. *Journal of the Taiwan Institute of Chemical Engineers* **2016**, *60*, 59–75.